Heteroleptic trivalent chromium in coordination chemistry: Novel building blocks for addressing old challenges in multimetallic luminescent complexes

Jimenez, Juan; Doistau, Benjamin; Poncet, Maxime Arnaud; Piguet, Claude

How to cite

JIMENEZ, Juan et al. Heteroleptic trivalent chromium in coordination chemistry: Novel building blocks for addressing old challenges in multimetallic luminescent complexes. In: Coordination Chemistry Reviews, 2021, vol. 434, n° 213750. doi: 10.1016/j.ccr.2020.213750

This publication URL: https://archive-ouverte.unige.ch/unige:149824
Publication DOI: 10.1016/j.ccr.2020.213750

Publication: *Coord. Chem. Rev.* **2021**, *434*, 213750. DOI: 10.1016/j.ccr.2020.213750

Heteroleptic trivalent chromium in coordination chemistry: novel building blocks for addressing old challenges in multimetallic luminescent complexes.

Juan-Ramón Jiménez,* Benjamin Doistau,* Maxime Poncet and Claude Piguet*

Department of Inorganic and Analytical Chemistry, University of Geneva, 30 quai E. Ansermet, CH-1211 Geneva 4, Switzerland.

Emails: Juan.JimenezGallego@unige.ch, Benjamin.Doistau@unige.ch, Claude.Piguet@unige.ch

Table of contents

Abstract

Although less famous than low-spin trivalent cobalt found in $[Co^{III}(NH_3)_{6-x}Cl_x]Cl_{3-x}$ ($x \leq 3$), which was exploited by Alfred Werner during the early part of the 20th century for establishing the basic rules of coordination chemistry, related trivalent chromium complexes exhibit comparable kinetic inertness, a rare property along the 3d-transition series. The associated slow isomerisation processes are compatible with the isolation of well-defined heteroleptic complexes. Some subtle energetic differences between Cr^{III}-X (X = halide, pseudo-halide, cyanide, solvent) and Cr-N bonds can be exploited for preparing stable and inert *cis*/*trans*-$[Cr(N^{\frown}N)_2X_2]^+$ and *fac*/*mer*-$[Cr(N^{\frown}N^{\frown}N)X_3]$ primary heteroleptic complexes incorporating multidentate nitrogen-containing chelate ligands. The use of these building blocks within the frame of the 'complex-as-ligand' strategy, or via the labilization of the remaining Cr-X bonds pave the way for the design of discrete polymetallic assemblies in which the photophysically appealing $[Cr^{III}N_6]$ chromophores could find applications as functional light-converting devices.

1. Introduction

The French naturalist-chemist-pharmacist Louis Nicolas Vauquelin made important contributions to chemistry and biology with the discovery of beryllium, chromium, asparagine, pectin, malic acid, to name a few. In 1797, Vauquelin isolated trivalent chromium oxide (Cr_2O_3) by reacting mineral crocoite ($PbCrO_4$) with hydrochloric acid. Subsequently, he was able to reduce Cr_2O_3 into impure metallic Cr by heating the oxide with charcoal [1]. A century later, Victor Goldschmidt isolated pure elemental chromium through an aluminothermic process [2,3]. In the earth's crust, the main source of chromium is chromite ($FeCr_2O_4$) and to a lesser extent crocoite ($PbCrO_4$) and chromium oxide (Cr_2O_3). Its abundance is relatively high (estimated 0.0102% in mass percent in the earth crust's) and it is mainly located in South-Africa, Kazakhstan and India, these countries being the largest producers of chromium (82% of the total world production). Recycling chromium from the stainless-steel scrap is the main secondary source of this metal. Nowadays, chromium is a highly valuable metal in metallurgy (Cr is the main additive in stainless steel) because of its appealing physical properties such

as ductility, anti-corrosive properties and easy surface treatment [4]. Minerals based on chromium are also used as pigments [5]. Chromium can be present in several oxidation states with Cr^{VI}, Cr^{III} and Cr^{II} being the most common ones, but Cr^{V} and Cr^{IV} are also known despite their unstability with respect to disproportionation reactions. Cr(0) can be stabilized by using weakly electronegative and strong π-accepting ligands (e.g. CN^- and CO^-) [6]. Chromium in its maximum oxidation state (Cr^{VI}) is a highly oxidizing agent ($E°(Cr_2O_7^{2-}/Cr^{3+})$ = +1.33V vs SHE), which is classified as toxic and mutagenic and thus should be handle with care. On the other side, Cr^{II} complexes is prone to be oxidized under aerobic conditions to produce Cr^{III} ($E°(Cr^{3+}/Cr^{2+})$ = -0.41V vs SHE), the most stable oxidation state of the family of chromium compounds [6]. Trivalent chromium has been subject of intense activity in photophysics since the discovery of the first ruby lasers in 1960 by Theodore Maiman [7]. In particular, the photophysical and photochemistry of octahedral Cr^{III} complexes are among the most investigated of all transition metal complexes because of the rather inert character of these complexes in solution which allows direct correlation between the nature of the Cr^{III} coordination sphere and the electronic properties [8-18]. However, Cr^{III} coordination chemistry remains very basic because (i) its kinetic inertness is not compatible with the virtues of themodynamically-driven assembly processes and (ii) its long electronic relaxation time prevents NMR spectra to be recorded, thus making synthetic chemists essentially blind. In recent years, some innovative works demonstrated that chromium complexes may act as crucial partners for approaching modern chemical challenges such as the implementation of long-lived NIR luminescence in solution, photoredox catalysis, photoinduced hole injection in solar cells, sensitization of molecular-based light-upconverters and phototriggered NO release in biological systems [13,19]. Combined with the considerable amount of chromium found in the earth crust (*i.e.* its low price) [11], the latter scientific aspects contribute to a renewal of interest for mastering its coordination chemistry. This tutorial review will focus on the synthetic approaches leading to heteroleptic Cr^{III} complexes with adjustable absorption, emission and light-converting properties.

2. Coordination Chemistry of Cr^{III}: kinetic aspects [20,21].

The coordination chemistry of Cr^{III} complexes was already investigated by Alfred Werner by the end of 19th century [22]. His pioneer work on octahedral Co^{III}-ammonia compounds were also applied, to a lesser extent, to Cr^{III}-ammonia compounds. In fact, a part of its Nobel Lecture in 1913, was dedicated to the exchange of ammonia with water around Cr^{III} in $[Cr(NH_3)_{6-x}(H_2O)x]^{3+}$ [22]. It is therefore not a coincidence that the early works in coordination chemistry, including Jorgensen's and Blomstrand's theories, mainly involved octahedral Co^{III} and Cr^{III} complexes rather than other metal ions of the first transition metal series. Their respective electronic configurations d^6 (low spin) and d^3 correspond to maximized ligand field stabilization energies due to the (semi)-filling of the t_{2g} orbitals in octahedral geometry, which prevent ligand exchange or dissociation [20]. The associated slow ligand exchange rates ($k < 0.01$ s^{-1} at 25°C and 0.1 M) allow the monitoring of ligand exchange reaction by using conventional analytical techniques, a critical point at that time [20]. Nowadays, modern stopped-flow and NMR techniques, which allow to monitor faster ligand substitution or dissociation reactions, have widen the scope of kinetic studies including metallic cations with labile electronic configurations [23,24]. Historically, kinetic studies on coordination complexes reactions have been mainly focused on inert square-planar Pd^{II} and Pt^{II} complexes and octahedral Co^{III} and Cr^{III} complexes [25,26,27,28]. Later, the *trans*-effect, an important kinetic phenomenon that is thought to labilize the ligands that are *trans* respect to strong donors in square planar complexes, was discovered and attributed to Ilya Chernyaev [29]. Altogether, those discoveries fixed the cornerstone of the chemical reactivity in coordination complexes. In this review we will restrict our discussions to octahedral complexes pertinent to Cr^{III} metallic centres, though the discussion of square-complexes is undoubtedly rich and exciting [30,31,32].

2.1. Generalities on ligand substitution reactions in octahedral complexes

Ligand substitution in octahedral complexes can occur through Associative (A) or Dissociative (D) mechanisms, taken as the two extremes of the reaction pathways, with the formation of an intermediate state possessing either a reduced coordination number for A or an increased coordination number for D (left and central part of Figure 1). However, ligand substitution reactions often take place with only partial association and dissociation (with no clear-cut intermediate state) in a kind of concerted reaction for which the term of Interchange (I) mechanism has been proposed (Figure 1, right part) [20].

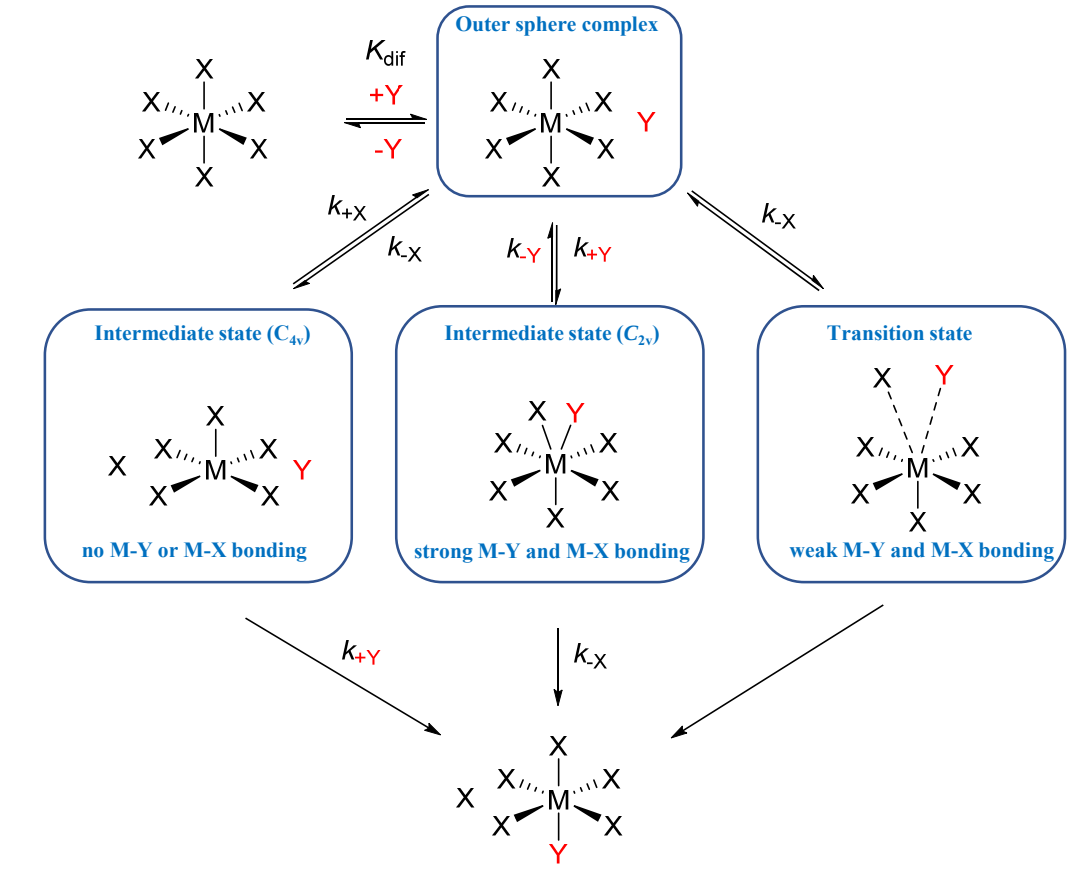

Figure 1. Possible ligand substitution mechanisms occurring in octahedral metal complexes and their kinetic constant (k_f) in the rate equation $V = k_f[MX_6][Y]$. Here, X corresponds to the leaving ligand and Y stands as the entering ligand [20].

This latter mechanism can also be partially associative (I_a), when the M-Y bond formation is more advanced than the M-X rupture in the transition state, or dissociative (I_d) when, in the transition sate, a considerable extension of an M-X bond is observed while an incipient interaction occurs with the incoming Y ligand. Figure 1 shows the different substitution reaction pathways taking into account the Eigen-Wilkins mechanism for a first encounter complex (outer sphere complex) with their respective intermediate and transition states where X is considered as the leaving group and Y is the entering group [20].

Table 1. Apparent reaction rate constants for water exchange (k_f), activation volumes ($\Delta V^{\ddagger}$), electron configurations and ionic radii for some transition metal hexa-aquo ions [6,20].

	k_f/ s^{-1}	$\Delta V^{\ddagger}$/ $cm^3 \cdot mol^{-1}$	Electron configuration	Ionic radius/ Å
V^{2+}	89	-4.1	t_{2g}^3	0.79
Mn^{2+}	$2.1 \cdot 10^7$	-5.4	$t_{2g}^3 e_g^2$	0.83
Fe^{2+}	$4.4 \cdot 10^6$	+3.7	$t_{2g}^4 e_g^2$	0.78
Co^{2+}	$3.2 \cdot 10^6$	+6.1	$t_{2g}^5 e_g^2$	0.74
Ni^{2+}	$3.2 \cdot 10^4$	+7.2	$t_{2g}^6 e_g^2$	0.69
Cu^{2+}	$4.4 \cdot 10^9$	2	$t_{2g}^6 e_g^3$	0.73
Ti^{3+}	$1.8 \cdot 10^5$	-12.1	t_{2g}^1	0.67
V^{3+}	$5.0 \cdot 10^2$	-8.9	t_{2g}^2	0.64
Cr^{3+}	$2.4 \cdot 10^{-6}$	-9.6	t_{2g}^3	0.61
Fe^{3+}	$1.6 \cdot 10^2$	-5.4	$t_{2g}^3 e_g^2$	0.65
Ga^{3+}	$4.0 \cdot 10^2$	+5	$t_{2g}^6 e_g^4$	0.62

To elucidate the reaction mechanisms of ligand exchanges, experiments based on the dependence of the reaction rate as a function of the temperature and pressure, taken separately, give access to the activation entropies ($\Delta S^{\ddagger}$), activation enthalpies ($\Delta H^{\ddagger}$) and activation volumes ($\Delta V^{\ddagger}$). The latter parameter is crucial because a negative value of $\Delta V^{\ddagger}$ unambiguously indicates the association between

the complex and the entering group into the transition state, the reverse being true for a positive value of $\Delta V^{\ddagger}$ which is taken as diagnostic for dissociative mechanisms. For instance, negative $\Delta V^{\ddagger}$ values are measured for water exchange in $[M(H_2O)_6]^{2/3+}$ with early 3d transition metals M = $V^{II}(d^3)$, high-spin $Mn^{II}(d^5)$ $Ti^{III}(d^1)$, $V^{III}(d^2)$, $Cr^{III}(d^3)$ and high-spin $Fe^{III}(d^5)$ implying associative mechanisms. On the contrary, positive $\Delta V^{\ddagger}$ values, characteristics for dissociative mechanisms, are found for water exchange occurring around $[M(H_2O)_6]^{2+}$ with high-spin $Fe^{II}(d^6)$, high-spin $Co^{II}(d^7)$ and $Ni^{II}(d^8)$ at the end of the 3d series (Table 1). The reaction rates constants for water exchange vary greatly within the first transition metal series (Table 1) and there is less systematic correlations between the charge (z) and the radius R with the kinetic rates through the *Born* factor z^2/R, as it is observed for alkali and alkali earth ions and other ions (s and p blocks) [33]. For instance, Cr^{2+} (d^4) and Cu^{2+} (d^9) are very labile ($k_f \geq 10^8$ s^{-1}), Cr^{3+} (d^3) is inert ($k_f \approx 10^{-6}$ s^{-1}), Mn^{2+} (d^5), Fe^{2+}(d^6), Co^{2+} (d^7) and Ni^{2+} (d^8) are labile ($k_f \geq 10^4$ s^{-1}) and V^{2+}, V^{3+} and Fe^{3+} ($k_f \approx 10^2$ s^{-1}) are intermediate [20]. On one hand, the very fast exchange around Cr^{2+} and Cu^{2+} (similar ionic radius than Ni^{2+}) can be assigned to the pronounced Jahn-Teller effect (half-filled e_g orbitals) that weakens the bonds with axial ligands. On the other hand, further rationalizations of the kinetic rates for the other 2+ and 3+ first row transition metals requires a correlation between exchange rates and d electron configurations (see below).

2.2. Effect of the d orbital electronic configurations: the case of Cr^{III}

In its ground state, the three valence electrons in an octahedral Cr^{III} complex (O_h symmetry) occupy the non-bonding degenerate d_{xy}, d_{xz} and d_{yz} orbitals ($t_{2g}(\pi)$ symmetry), while the antibonding d_z^2 and $d_{x^2-y^2}$ orbitals ($e_g(\sigma)$ symmetry) are empty (Figure 2a). Considering an octahedral geometry where the ligands act as point charges located along the cartesian axes around Cr^{III}, the half-filled t_{2g} orbitals are directed along the bisecting lines of the x, y, and z directions, far away from the point charge ligands (Figure 2b). Thus, the entering ligands (Lewis bases) should have difficulties to approach the Cr^{III} centre according to an associative mechanism. Moreover, the Crystal-Field Stabilization Energy (CFSE) is maximum for a d^3 configuration (t_{2g}^3 gives CFSE = $-1.2\Delta_{oct}$) with no electron occupying

the antibonding e_g orbitals (Figure 2a). Thus a dissociative pathway, which requires bond breaking, will be energetically costly.

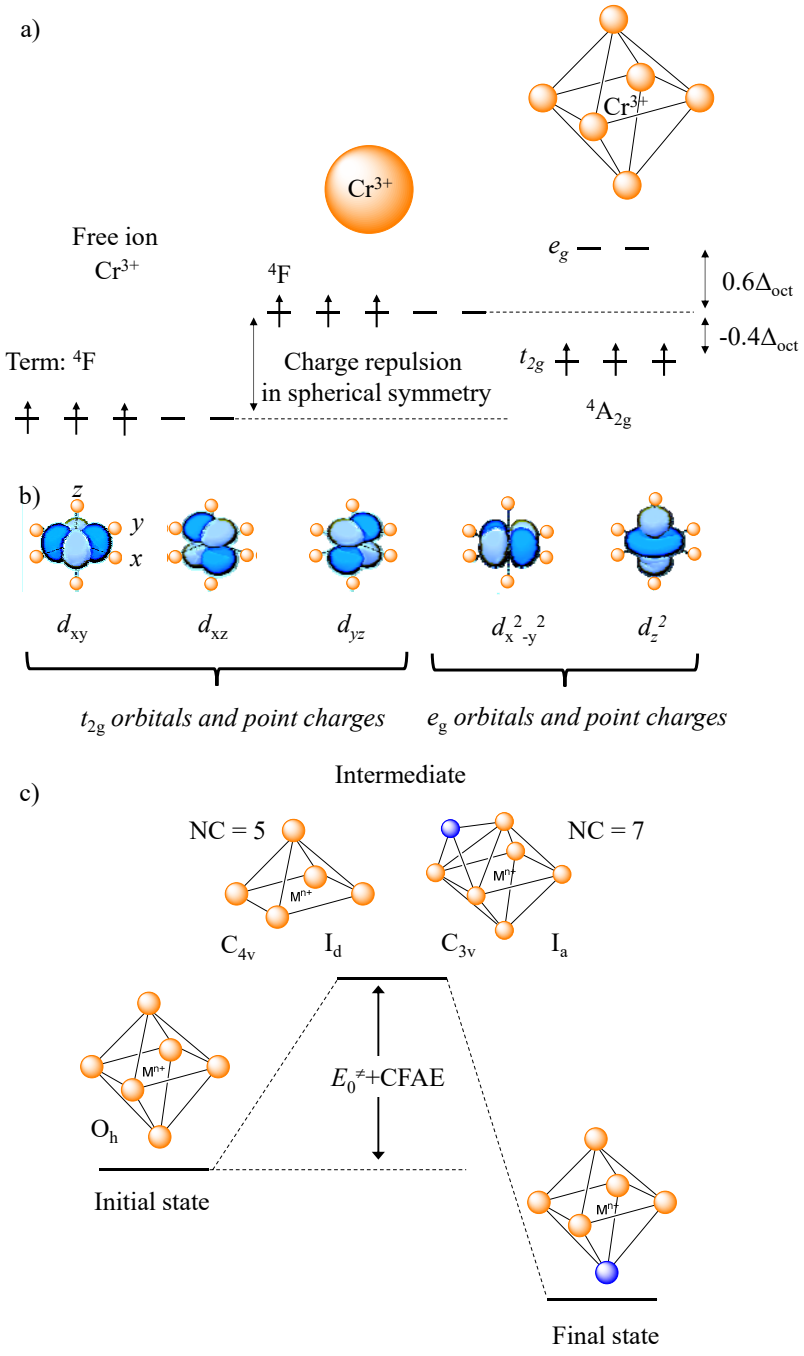

Figure 2. a) Splitting of the d-orbital for a Cr^{3+} cation in an octahedral crystal field. b) Spatial representation of the five d orbitals (d_{xy}, d_{xz}, d_{yz}, d_z^2 and $d_{x^2-y^2}$) embedded into an octahedral point charge model (orange spheres). c) Energy diagram for a ligand substitution reaction around an octahedral complex following an interchange mechanism (I_a (or A) or I_d (or D)). The blue sphere represents the entering ligand.

A semi-quantitative approach considers the Crystal-Field Activation Energy (CFAE), which is defined as CFAE = CFSE(activated complex) – CFSE(initial complex) for estimating the activation energy, where octahedral symmetry is assigned to the initial complex, while the activated complex adopt either square pyramidal (C_{4v}, D or I_d mechanism) or monocapped trigonal prismatic (C_{3v}, A or I_a mechanism) geometries (Figure 2c) [34]. The largest computed CFAE values correspond to the greatest inertia for the complexes (Table 2) and CFAE = 0.2 Δ_{oct} (dissociative) and CFAE = 0.18 Δ_{oct} (associative) computed for Cr^{III} complexes (d^3; Table 2, entry 3) are only overpassed by those of low-spin Co^{III} (d^6; Table 2, entry 6), which supports high kinetic inertness with a slight preference for A or I_a mechanisms when relevant for ligand exchanges around Cr^{III}.

Table 2. Crystal-Field Activation Energy (CFAE in units of Dq with Δ_{oct} = 10 Dq) for d^n electronic configurations using octahedral geometry for the initial complexes and square pyramidal (D mechanism) or monocapped trigonal prismatic (A mechanism) geometries for the activated complexes [34].

	Strong field (low spin)		Weak field (high spin)	
d^n	Dissociative	Associative	Dissociative	Associative
1	-0.57	-2.08	-	-
2	-1.14	-0.68	-	-
3	2	1.8	-	-
4	1.43	-0.26	-3.14	-2.79
5	0.86	1.14	0	0
6	4	3.63	-0.57	-2.08
7	-1.14	-0.98	-1.14	-0.68
8	2	1.8	-	-
9	-3.14	-2.79	-	-

2.3. Ligand effect on the reaction rates

According to Tables 1 and 2, ligand substitutions in Cr^{III} complexes occur preferentially via associative mechanisms (A or I_a), for which the rate constant depends on the nature of both the entering group and leaving group. For interchange associative reactions, the effect of the leaving group depends on the extent of bond breaking in the transition state. Generally, the stronger the bond with the leaving group in the initial state, the slower the substitution. This observation is at the origin of a correlation between thermodynamic and kinetic trends since strongly negative bond enthalpies ($\Delta H_{M\text{-}L}$ in the initial state) increase the activation energy and reduce the reaction rate. Leaving ligands possessing a strong σ donor and π acceptor characters located at the end of the spectrochemical series (such as heterocyclic nitrogen donors or cyanide anions) will tend to stabilize the initial complex by an increase of the ligand field splitting [35] and consequently the activation energy. On the other side, entering ligands with strong σ donor and π acceptor character tend to stabilize the intermediate state and thus reduce the activation energy of the interchange mechanism. The reaction rate can be also affected by the "spectator ligand" in proportion to the strength of the bonds they form with the metal atom. For instance, the hydrolysis reaction $[CrX_5Y] + H_2O \rightarrow [CrX_5(H_2O)] + Y$, is much faster when $X = NH_3$ than when $X = H_2O$. The stronger σ donor character of NH_3 increases the electron density at the metal (= reduces its formal positive charge) and thus facilitates the rupture of the M-Y bond during the interchange mechanism. The presence of *steric hindrance* by introducing didentate and tridentate ligands or voluminous monodentate ligands also inhibit somehow associative mechanisms because the entering ligand will experiment difficulties to approach the metal centre. For instance, in heteroleptic complexes such as $[Cr(N\frown N\frown N)X_3]$, where N⌒N⌒N is a tridentate chelate ligand, the substitution of the monodentate X groups will be favoured when the size of the entering ligands is minimum. Furthermore, the *chelate effect* provided by multidentate ligands is an important thermodynamic effect that also hampers their displacement compared to monodentate ligands. Finally, the presence of H^+, OH^- or metal ions can assist and accelerate the reaction rate (*acid and base catalysis)*. For instance, substitution of monodentate ligands in acid solutions in $[CrX(H_2O)_5]^{2+}$

have been demonstrated to be faster than under neutral conditions. In a first step, X is (partially) protonated, thus affording the $[(H_2O)_5Cr\text{-}XH]^{3+}$ species. The protonation weakens the Cr-X bond and facilitates the X extraction as HX in a proton-assisted substitution reaction. In basic medium, the presence of OH^- can also greatly accelerate the ligand substitution when co-ligands such as NH_3, RNH_2 or R_2NH, bound to the metal centre, contain acidic hydrogen atoms that might be deprotonated. In the following reaction: $[Co(NH_3)_5Cl]^{2+} + OH^- \rightarrow [Cr(NH_3)_5OH]^{2+} + Cl^-$, the reactive intermediate $[Cr(NH_2)(NH_3)_4Cl]^+$ indeed contains the NH_2^- amide group, a strong π donor which accelerates the Cl^- release. The associated rate law $V = k[Co(NH_3)_5Cl][OH]$ demonstrates the importance of $[OH]^-$ on the reaction rate. This mechanism is referred to as "mechanism of the internal conjugated base'' [36]. When the ammonia co-ligands (NH_3) are replaced with pyridine or tertiary amine, which have no available acidic protons, the basic hydrolysis is slower and may follow variable mechanisms (see section 2.4). For example, in alkali media, the complexes *mer*-$[Cr(pic)_3]^0$ and $[Cr(ox)_2(pic)]^{2-}$ (pic = 2-picolinate, ox = oxalate) undergo slow and successive ligand dissociations. The rate determining step corresponds to the breaking of a Cr-N bond for *mer*-$[Cr(pic)_3]^0$ and and of Cr-N and Cr-ox bonds for $[Cr(ox)_2(pic)]^{2-}$. In both cases, the rate constants were found to be almost independent of $[OH^-]$ [37]. Closely related examples have also been studied and reported [38-43]. An additional remarkable example concerns the $[Cr(lutH)_n(H_2O)_{6-2n}]^{3-n}$ complexes (where lutH- is the didentate N,O- bonded lutidinic acid anion). In acidic media, $[Cr(lutH)_3]^0$ undergoes only one ligand dissociation whereas, under alkaline treatment, the successive decomplexation of the three ligands generates chromate(III) (*i.e.* oxyanion of chromium in oxidation state 3). In acidic medium, the reaction takes place in two steps: (i) chelate-ring opening (Cr-N/O bond breaking) and (ii) ligand dissociation. In basic media, only the two first ligand dissociations depend on $[OH^-]$ while the kinetics of the last ligand liberation (from $[Cr(lut)(OH)_4]^{3-}$) seems to be $[OH^-]$ independent [44].

2.4. The lability of some octahedral polypyridyl Cr^{III} complexes in OH^- media

It has been also shown that strong alkali media can promote fast ligand exchange around octahedral Cr^{III} complexes in absence of deprotonable co-ligand in the first coordination sphere [45,46,47]. The archetypal $[Cr(bpy)_3]^{3+}$ (bpy = 2,2'-bipyridine) and $[Cr(tpy)_2]^{3+}$ (tpy = 2,2';6,2''-terpyridine) are indeed substitutionally labile under alkaline conditions and eventually give hydroxo complexes in aqueous solution (eqs 1-2) [14,46].

$$[Cr(bpy)_3]^{3+} + 2\ OH^- \rightarrow [Cr(bpy)_2(OH)_2]^+ + bpy \quad (1)$$

$$[Cr(tpy)_2]^{3+} + 3\ OH^- \rightarrow [Cr(tpy)(OH)_3] + tpy \quad (2)$$

Possibly, the π-accepting ligands bpy and tpy reduce the electron density of the Cr^{III} via π backbonding from t_{2g} orbitals. This removes electronic density from t_{2g} orbitals and favours an associative mechanism where a seven coordinate intermediate undergoes deprotonation at high pH, followed by loss of one ligand according to reactions 1 and 2 [48,49]. Upon light excitation, Cr^{III} complexes are also able to undergo photochemical reactions and, solutions of $[Cr(bpy)_3]^{3+}$ and $[Cr(tpy)_3]^{3+}$ undergo complete photosubstitution within a few hours [16,50].

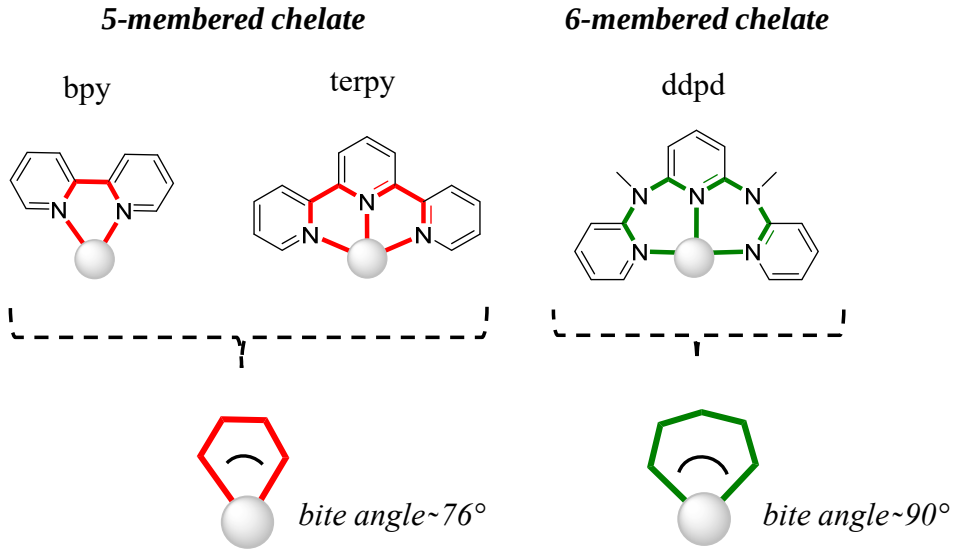

Figure 3. Representation of the bite angles provided by 5-membered chelate rings (bpy and tpy) and 6-embered chelate rings (ddpd).

In contrast, $[Cr(ddpd)_2]^{3+}$, where ddpd = N,N'-dimethyl-N,N''-dipyridin-2-ylpyridine-2,6-diamine is an electron rich ligand, is essentially inert in aqueous solution at high pH and under illumination

[14,51]. The ddpd ligand provides large N-Cr-N bite angles of ~90°/~180° which lead to strong ligand field splitting and poorly distorted octahedral geometries compared to bpy and tpy (Figure 3). Altogether, this structural and electronic improvement provided by the introduction of tuned ligands enhances the global stability and inertness of the Cr^{III} centre. Moreover, the large ligand-field splitting found for $[Cr(ddpd)_2]^{3+}$ suppressed the back intersystem crossing from the low-lying excited states, which is known to populate the reactive Jahn-Teller distorted $^4T_{2g}$ ($t_{2g}^2e_g^1$) state in $[Cr(bpy)_3]^{3+}$ and $[Cr(tpy)_3]^{3+}$.

2.5. Stereoisomers and stereochemistry of substitution in octahedral complexes

Kinetics is as important as thermodynamics in preparative coordination chemistry since the huge numbers of isomers of the octahedral Co^{III} and Cr^{III} complexes, and square-planar Pt^{II} complexes, could not have been isolated and structurally characterized if ligand exchange and racemization were fast. Structural isomerism in Cr^{III} complexes can be illustrated for $CrCl_3 \cdot 6H_2O$ which exists as three differently coloured hydration isomers: violet $[Cr(H_2O)_6]Cl_3$, pale green $[CrCl(H_2O)_5]Cl_2 \cdot H_2O$, and dark green $[CrCl_2(H_2O)_4]Cl \cdot 2H_2O$. These three hydrate isomers, as Alfred Werner called them, could be isolated in the solid state thanks to slow H_2O/Cl exchange that permit the trapping of each possible ligand arrangement around Cr^{III} as kinetic products [6]. Moreover, the concept of geometrical and optical stereoisomers occupies a very special place in coordination chemistry since Werner's theory was in part demonstrated by his predictions of stereoisomerism occurring in metal complexes [22]. Let us focus on six-coordinate Cr^{III} complexes where the chromium cation is put at the centre, and the six bound donor atoms occupy the six vertices of an octahedron (Figure 4a). No stereoisomerism is possible for $[CrX_6]^{3+}$ (O_h symmetry) and for $[CrX_5Y]^{3+}$ (C_{4v} symmetry) since interchanging the X and Y positions leaves the structure unchanged. Geometrical isomers arises with complexes of the type $[CrX_4Y_2]^{3+}$ illustrated by the *trans*-$[Cr(NH_3)_4Cl_2]^+$ (D_{4h} symmetry, Figure 4b) and *cis*-$[Cr(NH_3)_4Cl_2]^+$ complexes (C_{2v} symmetry, Figure 4c). Complexes of type $[CrX_3Y_3]^{3+}$ also have two geometrical isomeric forms with meridional (*mer*) and facial (*fac*) arrangements that can be illustrated by the *mer*-$[Cr(NH_3)_3Cl_3]$ (C_{2v} symmetry, Figure 4d) and *fac*-$[Cr(NH_3)_3Cl_3]$ complexes (C_{3v}

symmetry, Figure 4e). In the *fac* form, the three bound chloride or ammonia ligands are located at the corners of a face of the octahedron surrounding the metal ion, whereas in the *mer* isomer, three of those groups lie in a plane at right angles to the plane of the other three and passing through the metal atom. With chelating ligands, the situation is different and saturated homoleptic $[Cr(X^{\frown}X)_3]^{3+}$ complexes (D_3 symmetry, X⌒X stands for didentate symmetrical neutral chelating ligand) do not possess symmetry elements of the second kind and exist as pairs of *Δ* or *Λ* enantiomers (Figure 4f). Similarly, the heteroleptic complexes *cis*-$[Cr(X^{\frown}X)_2Y_2]$ (C_2 symmetry, Figure 4g) also exist as a pair of *Δ* or *Λ* enantiomers, while *trans*-$[Cr(X^{\frown}X)_2Y_2]$ belongs to C_{2v} point group with no enantiomer. A further increase in the number of possible isomers arises when the didentate ligand X⌒X' is non-symmetrical, but this discussion is beyond the scope of this review.

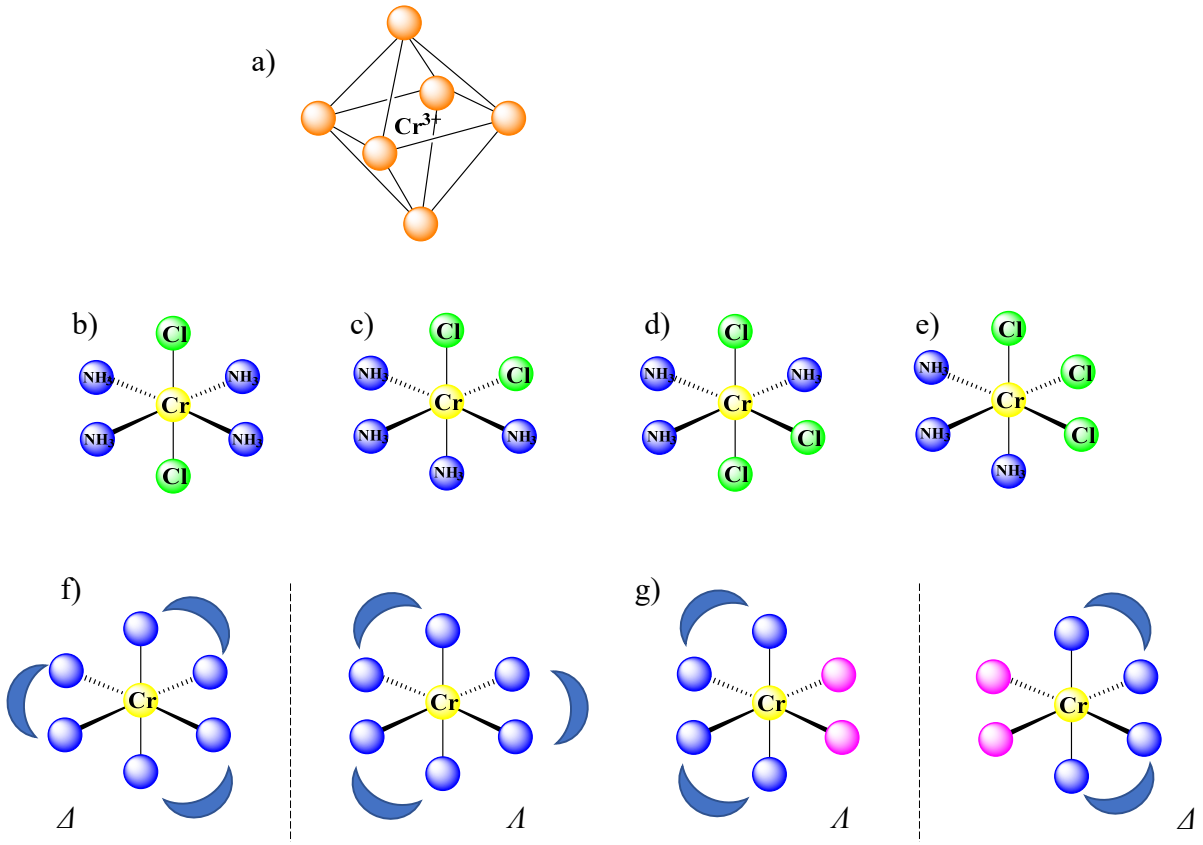

Figure 4. a) Octahedral Cr^{III} complexes and various stereoisomers: b) *trans*-$[Cr(NH_3)_4Cl_2]^+$, c) *cis*-$[Cr(NH_3)_4Cl_2]^+$, d) *mer*-$[Cr(NH_3)_3Cl_3]$, e) *fac*-$[Cr(NH_3)_3Cl_3]$, f) $[Cr(X^{\frown}X)_3]^{3+}$ and g) *cis*-$[Cr(X^{\frown}X)_2Y_2]^{3+}$.

With all these structural and geometrical isomers in mind, the stereochemistry of substitution reactions operating in octahedral complexes is expected to follow various mechanistic pathways often leading to mixtures of isomers [6],[20]. This can be illustrated for the dissociative (D) aquation reaction operating in inert *cis* and *trans*-$[Co(en)ClX]^+$ complexes (en = ethylenediamine, X = spectator ligand with tuneable trans-effect), where the intermediate species adopts a pentacoordinated geometry (Figure 5).

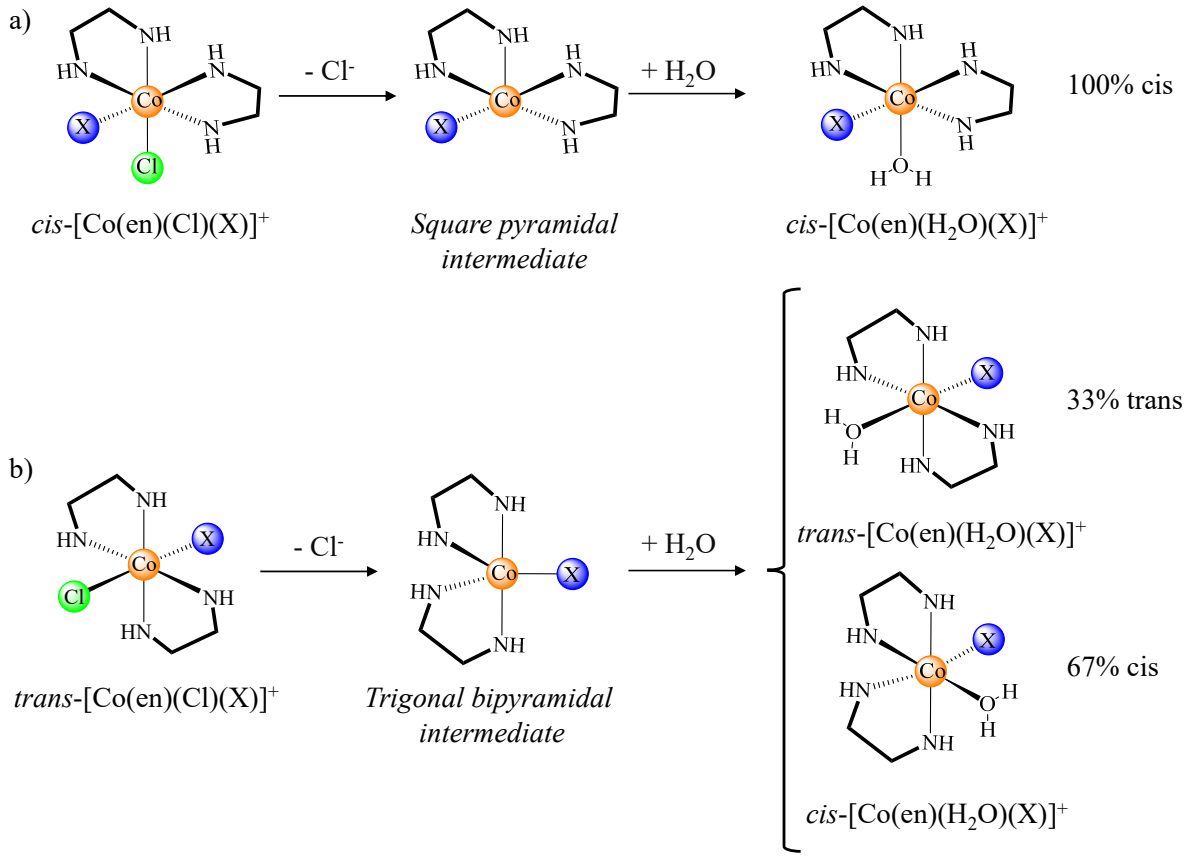

Figure 5. Stereochemistry of the substitution reaction of *cis* and *trans*-$[Co(en)ClX]^+$ following a dissociative pathway. Adapted from references [6] and [20].

For *cis*-$[Co(en)ClX]^+$, the chloride anion is located *cis* to the spectator ligand X and its dissociation produces a stable square-pyramidal intermediate with minor reorganization. The subsequent binding of a water molecule occurs with a complete retention of the configuration to give 100% of *cis*-$[Co(en)(H_2O)X]^+$ (Figure 5a). On the contrary, the dissociation of Cl^- from *trans*-$[Co(en)(Cl)X]^+$ leaves the spectator ligand without *trans* partner. A structural reorganization leads to a trigonal bipyramid intermediate, in which three vacant places in the equatorial plane are available for the

entering H_2O. This will lead to give a mixture of *cis* (probability = 2/3) and *trans* isomers (probability = 1/3; Figure 5b). These differences can be traced back to specific electronic π interactions between the ligands and the metallic centre in the two isomers [6]. Interestingly, the considerable structural rearrangement observed during the aquation of *trans*-$[Co(en)(Cl)X]^+$ results in a much slower kinetic rate constant compared its cisoid counterpart [20].

2.6. Inducing specific lability in kinetically inert complexes

The rate of ligand exchange occurring in the coordination sphere of an inert metal ion is strongly dependent on the nature of the bound ligands. In other words, one particular site in the coordination sphere may be more susceptible to undergo ligand exchange than others. For instance, if we consider the heteroleptic complex $[Cr(NH_3)_4(H_2O)_2]^{3+}$, the bound ammonia are generally less labile than bound water molecules because of the extra free electron pair in H_2O, which makes them more sensitive to attack by electrophilic groups. Thus, ammonia and amines in general can be considered as relatively inert or poor leaving groups compared to water. An alternative strategy for labilizing inert Cr^{III} complexes used the connection of weakly bound poorly coordinating anions such as $-OC1O_3^-$ (perchlorate) or $-OSO_2CF_3^-$ (triflate), from which the selective preparation of more sophisticated heteroleptic complexes can be programmed (eqs 3-4) [52,53].

$$[Cr(NH_3)_4Cl_2]^+ + 2HCF_3SO_3 \rightarrow [Cr(NH_3)_4(OSO_2CF_3)_2]^+ + 2HCl \uparrow \quad (3)$$

$$[Cr(NH_3)_4(OSO_2CF_3)_2]^+ + bpy \rightarrow [Cr(NH_3)_4bpy]^{3+} + 2\ CF_3SO_3^- \quad (4)$$

Following this strategy, the target heteroleptic complexes become accessible while the global kinetic inertness of the spectator ligands prevents ligand scrambling. This situation is rather unique for Cr^{III} along the 3d-block complexes and only the low-spin d^6 electronic configuration found in Co^{III} is comparable with the formation of inert heteroleptic complexes.

3. Synthetic strategies for the preparation of heteroleptic Cr^{III} complexes

Much efforts have been devoted to the exploration of reliable synthetic pathways dealing with the kinetic inertness of Cr^{III} ions, particularly for the preparation of well-defined heteroleptic Cr^{III} complexes. Their applications in many fields exploiting the magnetic, photophysical and

photochemical properties combined with the low cost of chromium metal made the search for new synthetic routes appealing.

3.1. Common strategies: from homoleptic toward heteroleptic Cr^{III} complexes

A common strategy initiates the complexation around labile Cr^{II} centres under an inert atmosphere and then oxidises the metal to give inert homoleptic complexes of Cr^{III} (Figure 6a,b left columns) [54]. Obviously, this technique cannot be applied for the synthesis of heteroleptic complexes of Cr^{III} because labile Cr^{II} complexes with different ligands exist as statistical mixtures in solution.

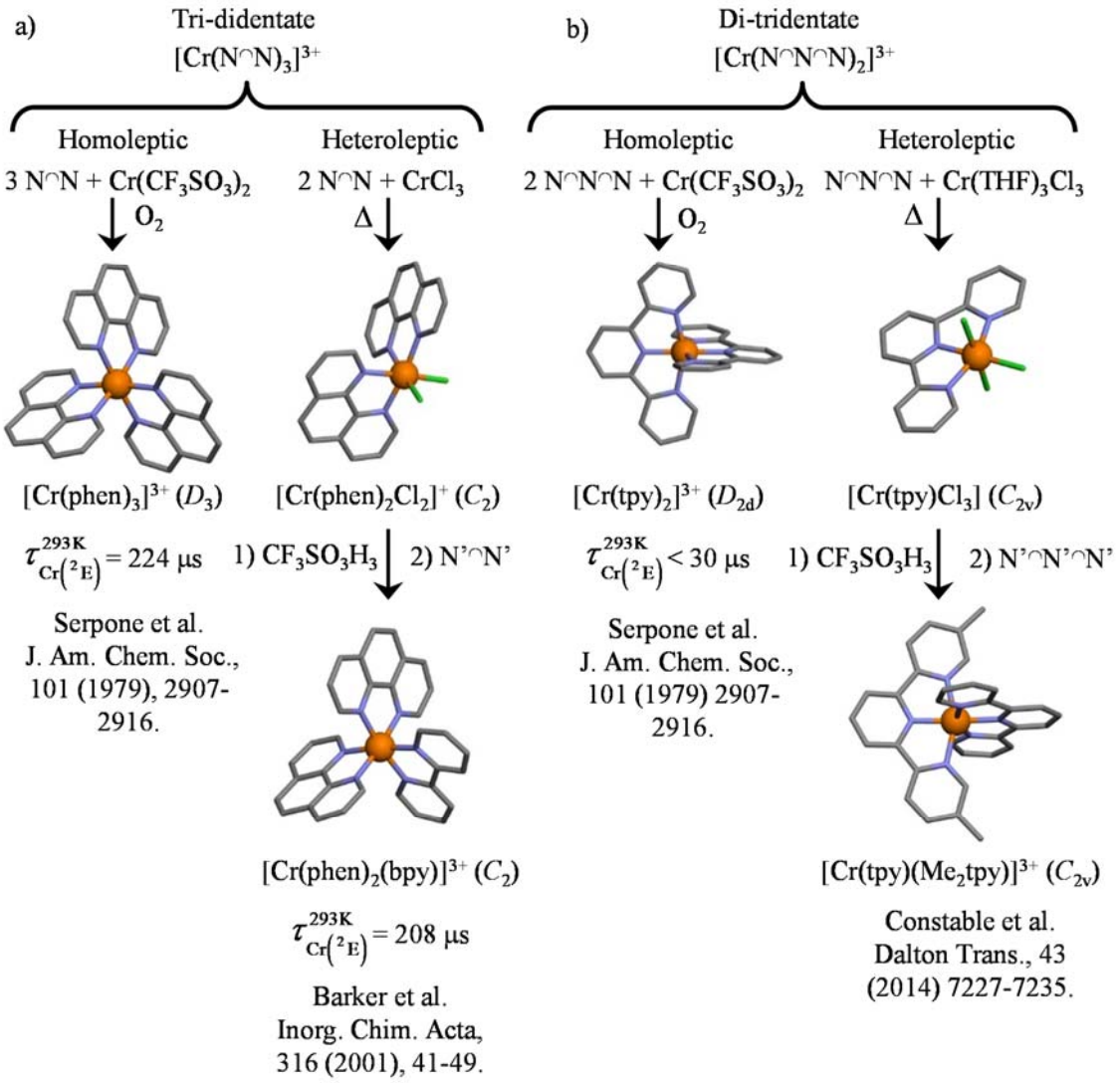

Figure 6. a) Synthetic pathways for the preparation of tri-didentate homoleptic $[Cr(phen)_3]^{3+}$ (left) [54] and heteroleptic $[Cr(phen)_2(bpy)]^{3+}$ (right) [55] b) Synthetic pathways for the preparation of di-tridentate homoleptic $[Cr(tpy)_2]^{3+}$ (left) [54] and heteroleptic $[Cr(tpy)(Me_2tpy)]^{3+}$ (right) [58]. Associated excited state $Cr(^2E)$ lifetimes at room temperature are included when reported.

Alternatively, the kinetic barrier to ligand exchange around Cr(III) can be overcome by heating, and simple CrX_3 salts (where X is a halogen) dissolved in ethanol or water solution are able to selectively substitute three solvent molecules with some entering ligands L to give the heteroleptic complex $[Cr(L)_nX_3]$ because Cr-Solvent bonds are much weaker than Cr-X bonds. In this context Kane-Maguire and co-workers described in 2001 an efficient three-step synthesis for the rational synthesis of heteroleptic $[Cr(diimine)_3]^{3+}$ complexes, which is denied of any ligand scrambling [55]. This technique is exploiting the lability of the weak $\{Cr\text{-}OSO_2CF_3\}$ bond [52,56]. Starting from CrX_3 (X = Cl or Br), two equivalents of a diimine ligand (N^N) are reacted at high temperature to give $[Cr(N^N)_2(X)_2]X$. An excess of trifluoromethanesulfonic acid (HCF_3SO_3) is then added to yield $[Cr(N^N)_2(CF_3SO_3)_2]CF_3SO_3$ with the release of HCl (see eq. 3). Further reaction with one equivalent of a different diimine ligand N'^N' in a non-coordinating solvent (such as CH_2Cl_2 or CH_3CN) upon moderate heating replaces the two labile bound triflates to give the heteroleptic complex $[Cr(N^N)_2(N'^N')](CF_3SO_3)_3$ (Figure 6a, right column) [55]. This technique was further improved in 2007 with three different diimine ligands and provided some rare $[Cr(N^N)(N'^N')(N''^N'')](CF_3SO_3)_3$ complexes [57]. More recently, the labile $[Cr(N^N)_2(CF_3SO_3)_2]^+$ complex was reacted with Ni(II) and Fe(II) tetrapyridylporphyrins to produce tetrachromated metalloporphyrins, which are active in flash photolysis, and where four heteroleptic Cr^{III} units are connected to the central macrocycle (Figure 7) [59].

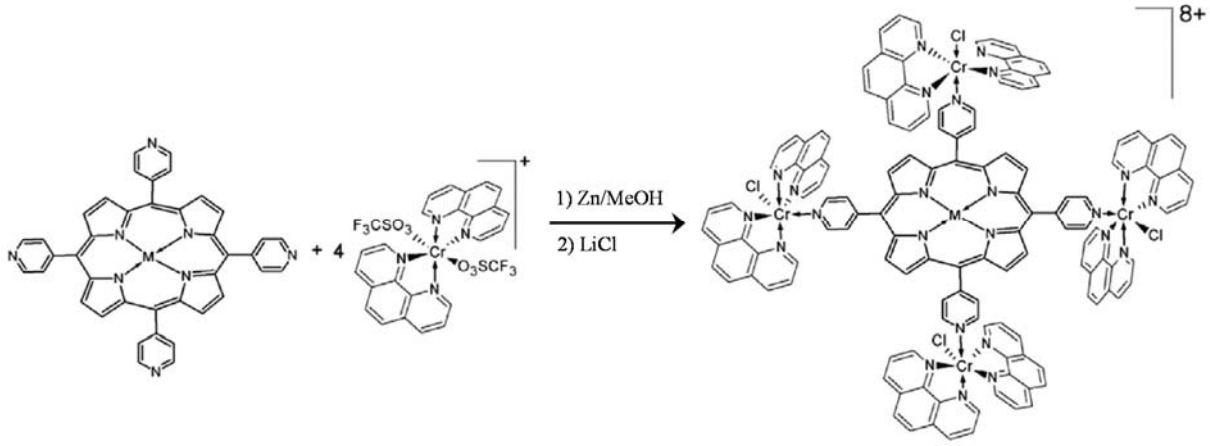

Figure 7. Synthesis of tetrachromated metalloporphyrins (M = FeII, NiII) [59].

3.2. Monodentate ligands

Heteroleptic complexes using monodentate ligands are much older and much simpler to prepare than those with multidentate ligands. One of the first reported heteroleptic complex is the Reinecke's salt that has the formula $NH_4[Cr(NCS)_4(NH_3)_2]$ [60]. However, this salt was isolated from natural extracts and there was no available synthetic methods before the beginning of the 20th century. The solubilisation of CrX_3 chromium salts in polar solvents followed by the coordination of an incoming ligand can be identified as the strategy of choice, which is applicable to a very wide range of monodentate ligands (for basic illustrations, see Figure 4b-e). An early example of this synthesis dissolved CrF_3 in water, while the subsequent addition of pyridine (pyr) in the mixture gave the heteroleptic complex $[Cr(pyr)_3F_3]$ [61].

3.3. Multidentate ligands

The most widely used didentate ligands for preparing Cr^{III} complexes in coordination chemistry are probably diamine or diimine chelators (N⌒N). This contrasts with the requirements of *Pearson*'s Hard and Soft Acids and Bases (HSAB) theory, which predicts a larger affinity of oxygen donors for Cr^{III} [62]. However, oxygen-containing didentate ligands have been also used to prepare homoleptic and heteroleptic complexes [63-64]. For instance, symmetrical O-donor ligands such as acetylacetonates or oxalates bound to Cr^{III} have found application in light-conversion [65,66]. On the other hand, Schiff-base ligands have been also useful in biology because of their bactericidal or antiviral activities [67], whereas more sophisticated 2,6-diacetylpyridine(semi-carbazone) ligands bound to Cr^{III} have been used as spin carriers in single-chain magnets [68,69]. The synthetic methodology applicable to multidentate ligands remains similar to that developed for monodentate ligands with the displacement of coordinated solvent molecules such as water or acetonitrile in a non-coordinating solvent (for instance dichloromethane) containing the entering ligand. This pathway leads to $[CrLX_3S]$ and $[CrL_2X_2]^+$ complexes depending of the initial Cr:L stoichiometry (L is a neutral didentate ligand, X is a (pseudo)-halogen and S is a solvent molecule). Wieghardt and co-workers extended this method for the selective binding of the di-tridentate dtne ligand (dtne = 1,2-bis(1,4,7-triaza-1-

cyclononyl)ethane) in the dinuclear *fac-fac* $[X_3Cr(dtne)CrX_3]\cdot H_2O$ (X = Cl, CO, Br) complex, where both chromium atoms are facially coordinated (Figure 8) [70]. Beyond the standard reaction of $CrCl_3\cdot 6H_2O$ with dtne in DMSO, at high temperature, a second strategy for X = CO, Br started with $[Cr^0(CO)_6]$ that was mixed with the dtne ligand to form $[(CO)_3Cr(dtne)Cr(CO)_3]\cdot H_2O$. This complex could be oxidized with Br_2 in a non-coordinating solvent to give $[Br_3Cr(dtne)CrBr_3]\cdot H_2O$. Inspired by this work and using the CO strategy, Kirk and Namasivayam prepared the analogous heteroleptic complexes $[Cr(tacn)X_3]$ where X = Br, F, NCS, CN, CO (tacn = 1,4,7-triazacyclononane, Figure 8) [16,17]. The more flexible tetradentate ligand tet (tet = N,N'-bis(2-aminoethyl-1,3-propanediamine), Figure 8) have been shown to be also compatible with the formation of heteroleptic Cr^{III} complexes. Reaction with $CrCl_3\cdot 6H_2O$ gave $[Cr(tet)Cl_2]^+$, which can be isolated either as the *trans* or *cis*-isomers under different empirical experimental conditions [71]. Alternatively, $Cr(NO_3)_3$ could be reacted with HF under reducing conditions in water to give *trans*-$[Cr(H_2O)_4F_2]^+$, which was then transformed into *trans*-$[Cr(pyr)_4F_2]^+$ under heating in pyridine. Final treatment with the tet ligand provided the heteroleptic complex $[Cr(tet)F_2]ClO_4$, also either as its *trans* or *cis* isomer [72].

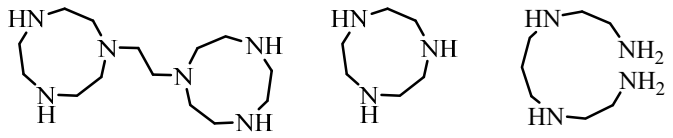

dtne tacn tet

Figure 8. Chemical structures of dtne (1,2-bis(1,4,7-triaza-1-cyclononyl)ethane), tacn (1,4,7-triazacyclononane) and tet (N,N'-bis(2-aminoethyl-1,3-propanediamine).

All these methods became less attractive after the introduction of the triflate ($SO_3CF_3^-$) pathway by Kane-Maguire at the beginning of this century (eqs 3-4) [55] because it proved to be safer, simpler and applicable to a wider range of ligands (Figure 6a,b right columns). However, the main downside concerns the strong acidic conditions associated with the treatment with triflic acid HSO_3CF_3 during the second step since some ligands are protonated, which prevents their coordination to the chromium atom. To overcome these limitations, Doistau and co-workers introduced a sacrificial base (pyridine or 2,6-lutidine) to quench the remaining acid from the previous synthesized intermediate which

allows the coordination of the entering ligand to Cr(III) [73]. Nevertheless, the triflic acid pathway was restricted for more than a decade to the design of heteroleptic tri-didentate $[Cr(N^{\frown}N)_x(N'^{\frown}N')_{3-x}]^{3+}$ complexes (Figure 6a, right column) [74].

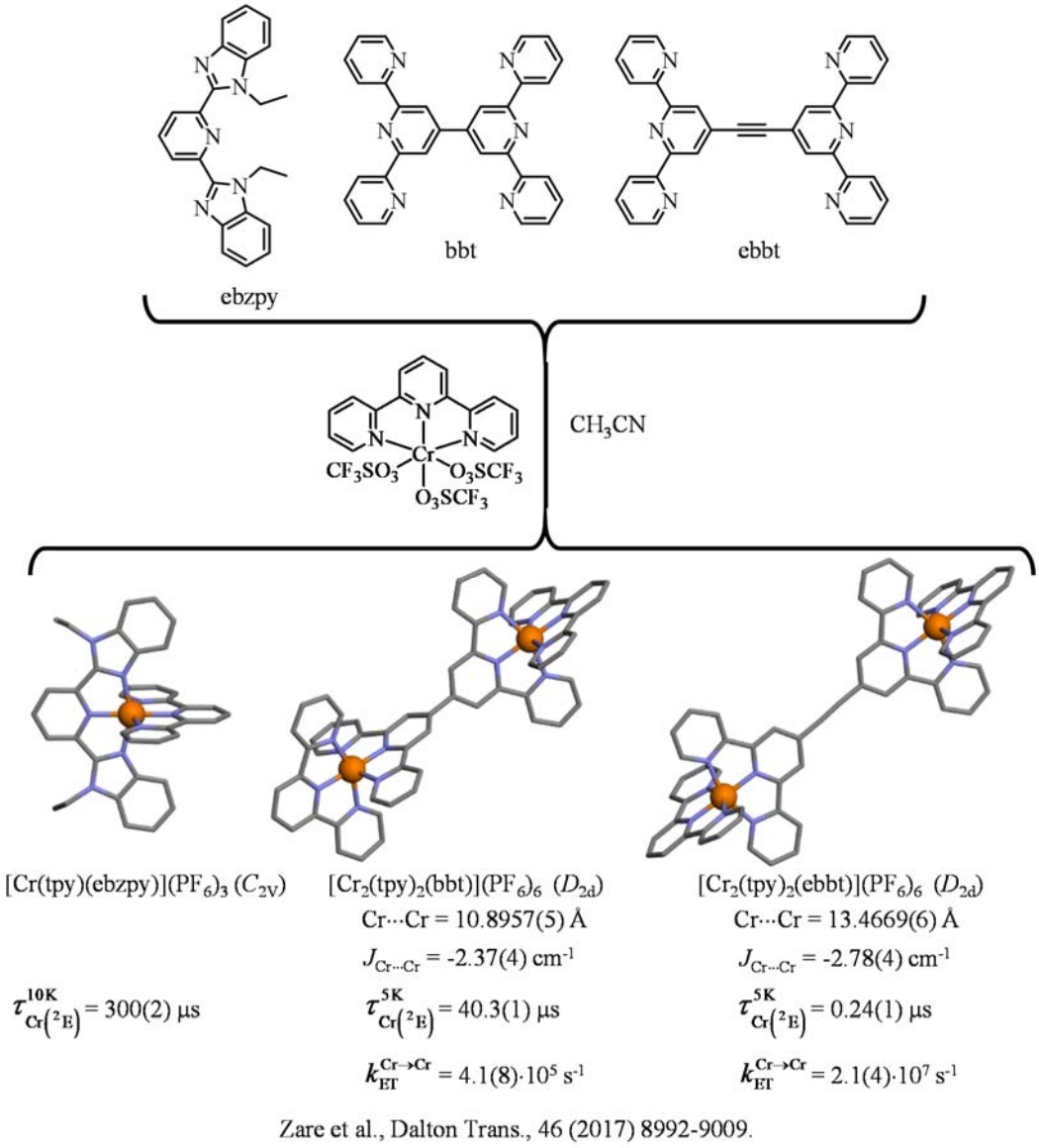

Figure 9. a) Synthetic pathways leading to heteroleptic mononuclear $[Cr(tpy)(ebzpy)](PF_6)_3$ and dinuclear $[Cr_2(tpy)_2(bbt)](PF_6)_6$, $[Cr_2(tpy)(ebbt)](PF_6)_6$ where ebzpy = 2,6-bis(1-ethyl-1*H*-benzo[*d*]imidazol-2-yl)pyridine, bbt = 6′,6″-di(pyridin-2-yl)-2,2′:4′,4″:2″,2‴-quaterpyridine and ebbt = 4′,4‴′-(ethynyl)bis(2,2′:6′,2″-terpyridine). Intermetallic magnetic coupling constants ($J_{Cr\text{-}Cr}$) and energy transfer rate constants $k_{ET}^{Cr\rightarrow Cr}$ are highlighted. Associated excited state Cr(^{2}E) lifetimes at room temperature are included [76].

Only in 2014, Constable, Housecroft and co-workers successfully extended this method for the synthesis of heteroleptic di-tridentate $[Cr(N^{\frown}N^{\frown}N)(N'^{\frown}N'^{\frown}N')]^{3+}$ complexes using fused five-membered tridentate chelates, the archetypal of which is 2,2':6',2"-terpyridine (tpy) [75]. As an early illustration, the reaction of $[Cr(tpy)Cl_3]$ with HSO_3CF_3 indeed produced the intermediate $[Cr(tpy)(CF_3SO_3)_3]$ which, upon mixing with 5,5‴-dimethyl-2,2':6',2"-terpyridine (Me_2tpy), yielded the heteroleptic complex $[Cr(tpy)(Me_2tpy)](CF_3SO_3)_3$ (Figure 6b, right column) [58]. With this toolbox in hand, terpyridine ligands could be replaced with analogous 2,6-bis(benzimidazol-2-yl)pyridine (Figure 9, left) and sophisticated luminescent heteroleptic dinuclear supramolecular assemblies $[(tpy)Cr(L)Cr(tpy)]^{6+}$ dyads (L = bridging ligand) displaying intramolecular intermetallic magnetic coupling and energy transfers could be isolated (Figure 9, centre and right) [76]. Inspired by the work of Goswami and co-workers [77], Jiménez and co-workers realized that triflic acid (HCF_3SO_3) can be replaced with silver triflate ($AgCF_3SO_3$) for helping in the labilization of the Cr-halogen bonds. The precipitation of AgX drives the substitution reaction to completion under neutral conditions, which makes the original Kane-Maguire strategy, originally limited to five-membered chelate rings (Figure 10 left) [78] compatible with the introduction of basic tridentate six-membered chelate rings (Figures 10 right and Figure 11) [79].

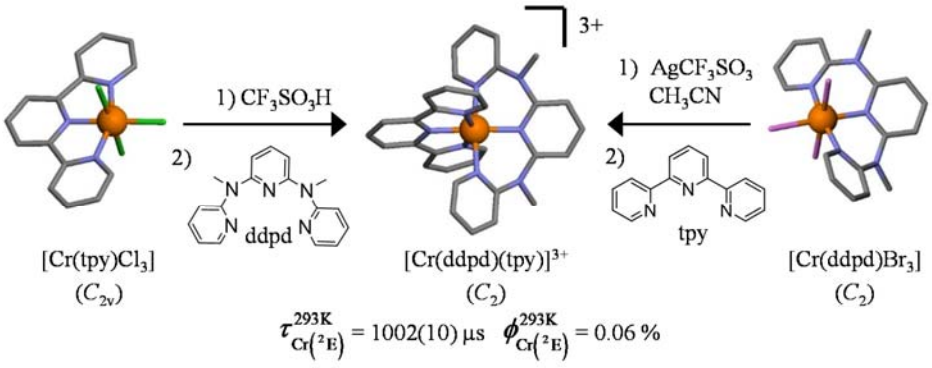

Figure 10. Synthetic pathways leading to the heteroleptic di-tridentate $[Cr(tpy)(ddpd)]^{3+}$ complex incorporating five-membered (tpy) and six-membered (ddpd) chelate rings. Associated excited state $Cr(^2E)$ lifetimes and quantum yields (ϕ) at room temperature are included [78].

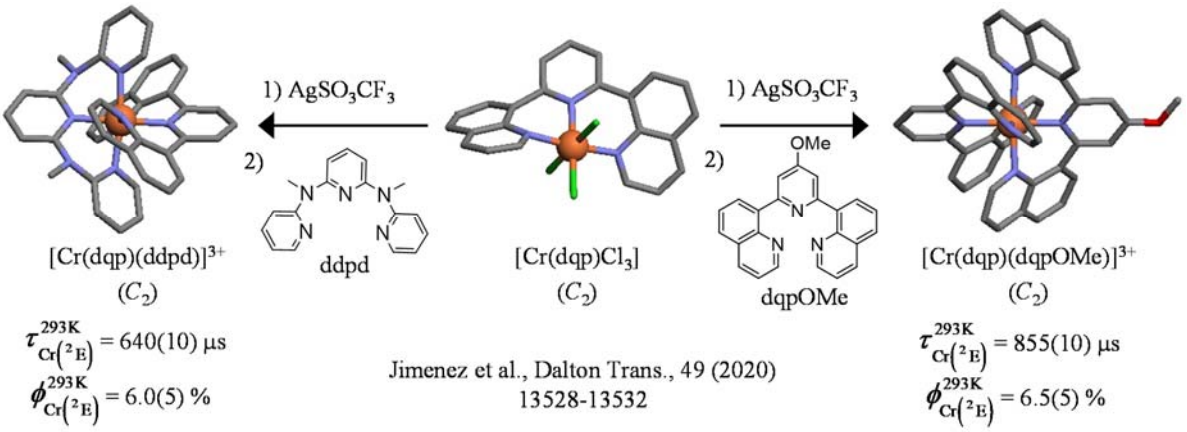

Figure 11. Synthetic pathways leading to the heteroleptic di-tridentate $[Cr(dqp)(ddpd)]^{3+}$ and $[Cr(dqp)(dqpOMe)]^{3+}$ complexes incorporating only six-membered chelate rings. Associated excited state $Cr(^2E)$ lifetimes and quantum yields (ϕ) at room temperature are included [79].

4. Heteroleptic Cr^{III} complexes in extended assemblies

4.1. Serendipitous assemblies under thermodynamic control

The incorporation of Cr^{III} in polymetallic architectures is particularly attractive for (i) designing multimetallic high spin molecules or single molecule magnets [80] and (ii) exploiting the photophysical features of activator/sensitizer systems made of Cr^{III}/Ln^{III} couples (Ln is a trivalent lanthanide) [81]. However, building Cr^{III}-containing (supra)molecular assemblies represents a considerable challenge regarding the chemical inertness of Cr^{III} complexes that prevents thermodynamic self-sorting under ambient conditions. The preparation of di- or tri-metallic complexes holding Cr^{III} chromophores therefore relied on the self-assembly of labile Cr^{II} followed by air oxidation (see point 3.1), but mainly homoleptic complexes could be obtained with this strategy. For more sophisticated polynuclear heteroleptic Cr^{III} complexes, the formation of intricate mixtures due to ligand scrambling, combined with the lack of thermodynamic control, prevent rational synthesis [82-90]. In this context, chemists invoked serendipity for exploring the lucky formation of the most stable and/or the most inert final species upon tremendous heating. The latter option was applied with success for the synthesis of remarkable clusters, cages and wheels. In their seminal work, Winpenny and co-workers first obtained several homometallic Cr^{III}-containing wheels upon heating at 400°C under solvothermal conditions (Figure 12) [80].

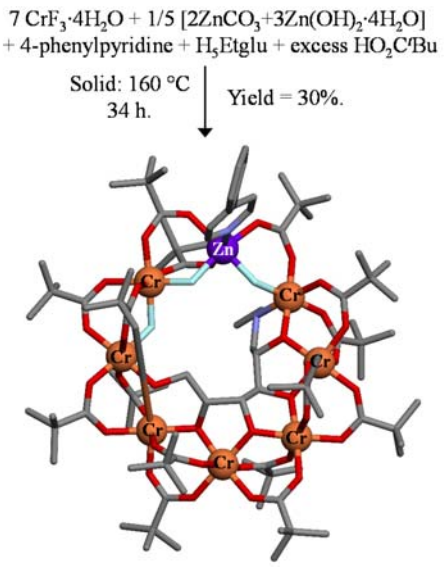

Figure 12. The serendipity approach to Cr^{III}-containing clusters showing the synthesis and crystal structures of $[Cr_7ZnF_3(Etglu)(O_2CBu)_{15}(4\text{-phenylpyridine})]$. Color code: C = grey, N = deep blue, O = red, F = light blue, Zn = violet, Cr = orange, [80].

The latter wheels were composed of eight repeating $[CrF(O_2C\text{-}R)_2]$ or $[Cr(OH)(O_2C\text{-}R)_2]$ (R = ^{t}Bu, Ph) units, coordinated by both bridging carboxylic acids, hydroxide and fluorine ligands. Subsequent work afforded an important diversity of homo- and heterometallic Cr^{III}-containing wheels, cages, chains or rotaxanes, of various sizes, the magnetic properties of which were extensively reported [80]. It is worth noticing that the Cr(III) complexes in those structures are homoleptic.

4.2. <u>The complex-as-ligand strategy</u>

The 'chemistry-on-complex' strategy pertinent to Ru^{II} coordination chemistry, which uses cross-coupling reactions operating on inert coordination complexes, could not be adapted to Cr^{III} because of the limited robustness of Cr^{III} complexes in basic or reductive media. Alternatively, some control of the final polynuclear chrome-containing architectures seems to be achievable if preformed inert Cr^{III} building blocks possessing free binding sites could be programmed for the subsequent coordination of additional metals according to the 'complex-as-ligand' strategy. Consequently, the common approach to Cr^{III}-containing extended assemblies relies on the connection of bridging

ligands to Cr^{III} centres in order to give primary mononuclear inert heteroleptic building blocks, which are then exploited for further complexation reactions (Figures 13-15). Because of the complexity of the Cr^{III} chemistry, the ditopic bridging ligands selected for the heteroleptic Cr^{III} building blocks are mainly restricted to monodentate cyanide (CN^-, Figure 13) [91-94], didentate oxalates (ox^{2-}, Figure 14) [95-99], and more recently tridentate polypyridyl ligands (Figure 15) [100].

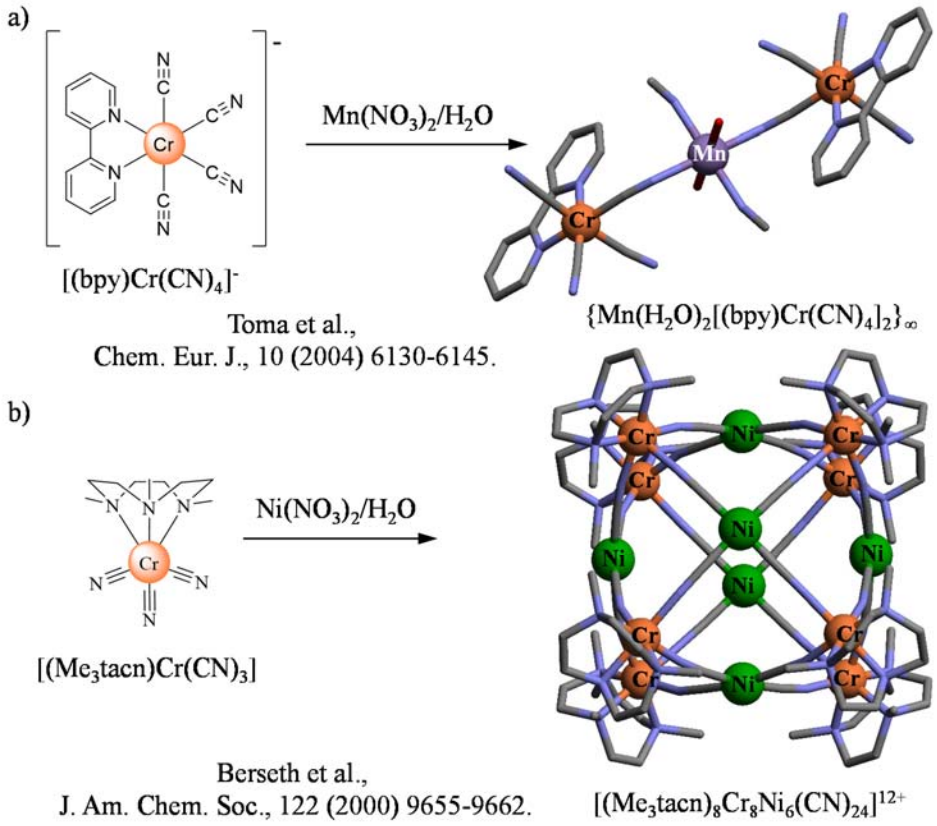

Figure 13. The complex-as-ligand approach using a) $[(bpy)Cr(CN)_4]^-$ and b) $[(Me_3tacn)Cr(CN)_3]$ building blocks [92-93]. Color code: C = grey, N = blue, O = red, Ni = green, Cr = orange, Mn = purple.

The short and conjugated cyanide ligand (CN^-) was implemented in polymetallic structures to promote strong magnetic coupling between metallic centres *via* a delicate ligand exchange mechanism. Among the possible $[Cr(N^{\frown}N)_x(CN)_{6-2x}]^{(2x-3)+}$ building blocks where N⌒N is a didentate N-donor chelate ligand, the complex $[Cr(N^{\frown}N)(CN)_4]^-$ (Figure 13a) was extensively exploited for the formation of polymetallic molecules, chains and networks often displaying SMM or SCM (single chain magnet) features [92]. The divergent four linear cyanide binding units make the latter complex

more adapted to the formation of polymeric entities. In addition, the coordination vectors and the weak binding affinity of bridging monodentate ligands hamper the control of the architecture design in solution and restrict the synthesis to serendipitous crystallisation processes.

Long and co-workers gave rise to an important breakthrough in the field of designed molecular Cr^{III}-containing structures when preparing the facial complex $[Cr(tacn)(CN)_3]$ (tacn = 1,4,7-triazacyclononane, Figure 13b). The latter building block (i) allows the formation of molecular entities with no competition with coordination polymers and (ii) permits self-sorting, upon using appropriate stoichiometry, due to the directionality of the three cyanide coordination vectors located within a controlled spatial cone. In addition to the original linear or prismatic clusters, the capping complex allowed the formation of more sophisticated molecular cubes, the vertices of which were composed of the $[Cr(tacn)(CN)_3]$ or $[Cr(Me_3tacn)(CN)_3]$ units [93]. Hence, in the $[Cr_4Co_4(CN)_{12}(tacn)_8]^{12+}$ cube, the similar Cr^{III} and Co^{III} capping building blocks occupy the vertices while the cyanides form the edges. In the extended face-centred cubic assembly $[Cr_8Ni_6(CN)_{24}(Me_3tacn)_8]^{12+}$, obtained by the mixing of $[Cr(Me_3\text{-}tacn)(CN)_3]$ with Ni^{2+} ions, the eight vertices are occupied by the $[Cr(Me_3\text{-}tacn)(CN)_3]$ complexes while the square planar $[Ni(NC)_4]^{2-}$ units form the faces of the cube (Figure 13b). Finally, in the largest version $[Cr_{12}Ni_{12}(CN)_{48}(Me_3\text{-}tacn)_{12}]^{12+}$, the Ni^{2+} cations are located on the edges connecting the $[Cr(Me_3tacn)(CN)_3]$ units. Although the work of Long and co-workers opens a route for the predictive formation of designed polymetallic architectures holding Cr^{III}, the control of self-organisation in solution and the monitoring of successive equilibrium remain tough or elusive [94].

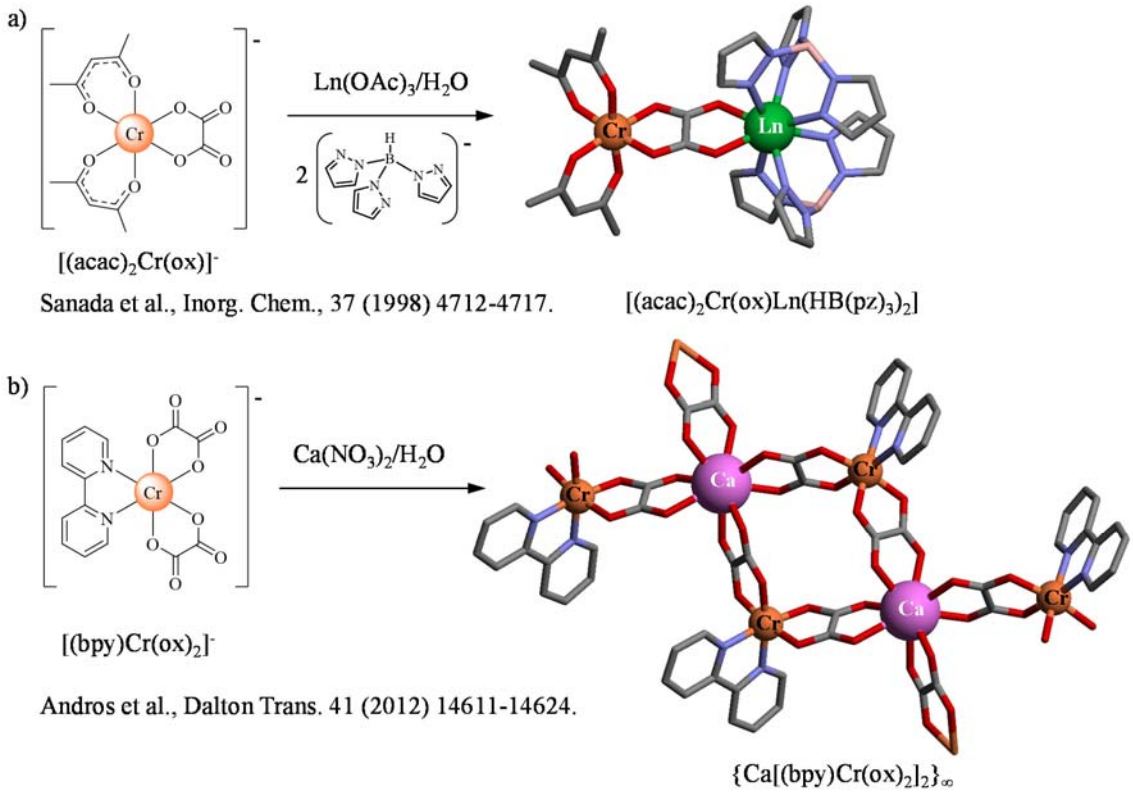

Figure 14. The complex-as-ligand approach using a) $[(acac)_2Cr(ox)]^-$ and b) $[(bpy)Cr(ox)_2]^-$building blocks. Color code: C = grey, N = blue, O = red, B = pale pink, Ln = green, Cr = orange, Ca = purple.

Alternatively, the oxalate-based building block $[(acac)_2Cr(ox)]^-$ has been extensively used by Kazaiki and co-workers as an optical partner for performing light-downshifting in dimetallic Cr-Ln dinuclear complexes, where the oxalate bridge ensures efficient intermetallic Cr↔Ln energy transfer processes (Figure 14a) [95-99]. The alternative mixed N/O building blocks $[Cr(N^{\frown}N)_x(ox)_{3-x}]^{(2x-3)+}$ (x = 1, 2) were developed in a view to harness the Cr^{III} magnetic properties in multimetallic high spin molecules or molecular magnets (Figure 14b) [100]. For such purpose, the short conjugated oxalate bridge promotes important exchange coupling and its coordination vectors favour ferromagnetic coupling, a crucial point for the implementation of single molecule magnet (SMM) behaviour. The $[Cr(N^{\frown}N)_2(ox)]^+$ building block is suitable to form controlled molecular polymetallic entities, since the presence of only one free binding site prevents polymeric network formation [101]. Conversely, the $[Cr(N^{\frown}N)(ox)_2]^-$ complex which holds two didentate binding sites allows network formation upon addition of metal ions, but the control of the design and stoichiometry of the formed architectures is

more elusive (Figure 14b). Despite the latter drawback the $[Cr(N^{\frown}N)(ox)_2]^-$ unit was probably the most exploited oxalato-based building block for the serendipitous synthesis and crystallisations of molecular entities and networks. In particular, Julve and co-workers were very active in implementing the complex-as-ligand strategy with the aforementioned oxalato-based building blocks. Hence the coordination in smooth conditions of $[Cr(N^{\frown}N)(ox)_2]^-$ to Cu^{II}, Mn^{III} and Mn^{II} afforded dinuclear, trinuclear and tetranuclear heterometalic complexes. Hexanuclear architectures were achieved by coordination of $[Cr(bpy)(ox)_2]^-$ to Pr^{3+}, and higher nuclearity was shown to be accessible in infinite chains, in 2D or in 3D networks [101]. In order to enable some rational programming and monitoring in solution, Doistau et al. designed a Cr^{III} building block, in which a $[Cr(phen)_3]^{3+}$ emissive moiety is connected through a rigid alkyne spacer to a (bis-benzimidazole)pyridine tridentate free binding unit (Figure 15) [102]. The latter unit displays some considerable binding affinities in solution for a large panel of transition metals and lanthanide cations. Interestingly, the successive binding equilibria can be monitored by NMR, an outstanding feature for Cr^{III} complexes since the slow electronic relaxation of the orbitally non-degenerate $Cr^{III}(^4A_2)$ ground state usually prevents any NMR analysis. In $[Cr(phen)_2(phen\text{-}bzpy)]^{3+}$ (Figure 15), the alkyne spacer is long enough to fix the free tridentate binding unit at a sufficiently long distance to limit the electronic-induced nuclear relaxation. The formation of dimetallic $[(phen)_2Cr(phen\text{-}bzpy)M(bzpy\text{-}phen)Cr(phen)_2]^{8+}$ ($M = Fe^{II}$, Zn^{II}) could be thus evidenced by using standard NMR techniques. The complex-as-ligand $[Cr(phen)_2(phen\text{-}bzpy)]^{3+}$ opens important perspectives for the incorporation of long-lived NIR $[Cr^{III}N_6]$ chromophores into polymetallic devices including optically appealing lanthanides.

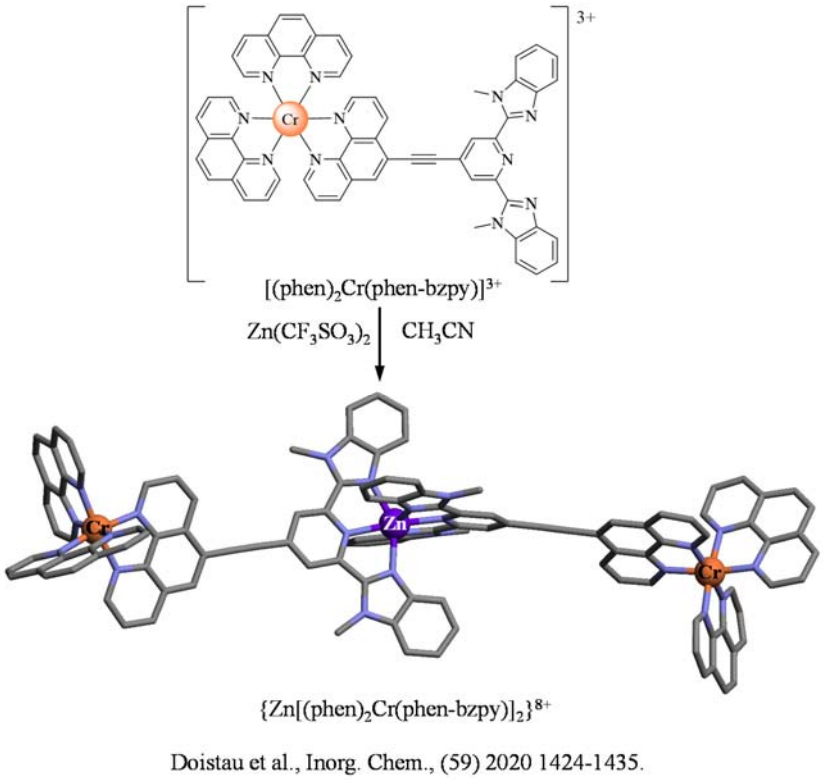

Figure 15. The complex-as-ligand approach using the $[Cr(phen)_2(phen\text{-}bzpy)]^{3+}$ building block (phen-bzpy = 2,6-bis(N-methyl-benzimidazol-2-yl)-4-((1,10-phenanthrolin-5-yl)ethynyl)pyridine)). Color code: C = grey, N = blue, Cr = orange, Zn = violet.

5. Photophysical properties of heteroleptic Cr^{III} complexes

The electronic properties of inert Cr^{III} complexes were studied in depth by Forster [8,63], Endicott [18] and Kirk [15,16], and they were originally thought as essential partners for photochemistry and photophysics. However, the report by Gafney and Adamson in 1972 [103] of a rare photoexcited electron transfer reaction involving the ^{3}MLCT state of $[Ru(\alpha,\alpha'\text{-diimine})_3]^{2+}$ was the catalytic event that lead to the refocus of the photochemical community on low-spin d^6 systems and estrangement from Cr^{III} systems [10]. It followed an extraordinary growth of photochemistry and photophysics with low-spin d^6 systems over the last decades [104-107]. The possibility to prepare efficiently inert heteroleptic Ru(II) complexes further allowed their introduction as luminescent building blocks in polynuclear (supra)molecular machines and devices [50,108-110]. The recent awareness that only earth abundant and cheap metallic centres are valuable candidates for being exploited for solar

technologies renewed the global interest towards Cr^{III} chromophores [11,14,19] and prompted the chemist to develop more efficient Cr^{III} emitters, in particular heteroleptic complexes that could be incorporated into polymetallic structures [70,71,111]. The enhancement of the photophysical features of new [$Cr^{III}N_6$] chromophores were particularly successful in the last years which render the Cr^{III} even more promising for the energy conversion purpose and technological applications [51,112,113].

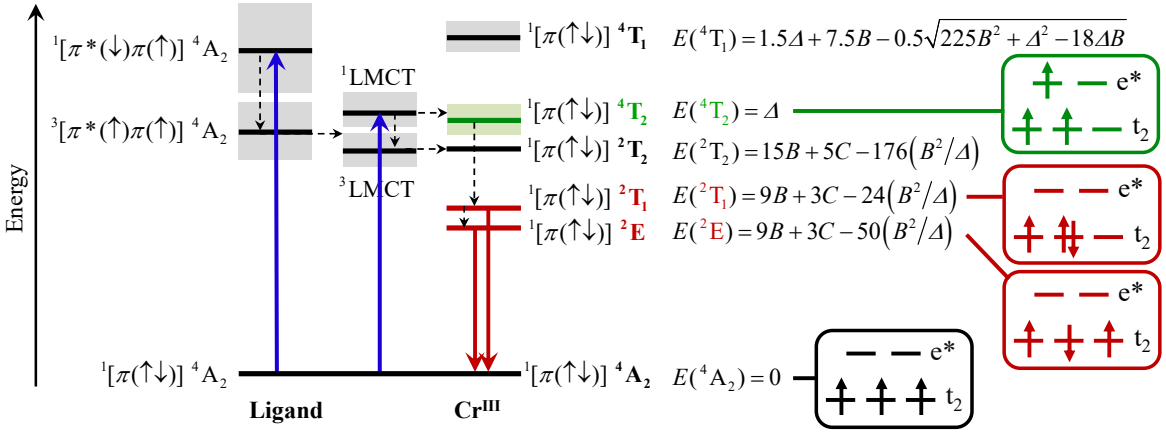

Figure 16. Perrin-Jablonski diagram showing the energy levels of the strong ligand field $Cr^{III}N_6$ chromophore (left), and the electronic structures associated to the low lying metal centred levels (right). The energy of the metal centred levels can be computed in terms of ligand field Δ and Racah parameter B and C [114].

The absorption spectrum of the target [$Cr^{III}N_6$] chromophores in Cr^{III} complexes, where N are heterocyclic nitrogen atoms, is dominated by strong ligand-centred transitions and ligand-to-metal charge transfer in the near ultraviolet to blue part of the electromagnetic spectrum, while less intense metal centred transitions are found in the visible to near infrared (NIR) domains. Contrary to the widely known Ru^{II}, Ir^{III} or Pt^{II} transition metal complexes that show intense ligand-centred or charge-transfer emissions [10], the narrow Cr^{III} dual emission, which occurs between 600 and 800 nm, arises from metal-centred spin flip transitions connecting the low lying and thermally equilibrated excited doublet levels $Cr^{III}(^2E)$ and $Cr^{III}(^2T_1)$, to the $Cr^{III}(^4A_2)$ ground state (Figure 16) [12]. The low-energy emission of d^3 Cr^{III} is scarce among the first-row transition metals since their low-energy metal-centred excited levels usually quench luminescence. This luminescence originates from (i) the nature of the spin flip $Cr^{III}(^2E \rightarrow {}^4A_2)$ d–d transition which is weakly coupled with vibration modes since only

low covalence is involved in the $Cr^{III}(^2E/^2T_1)$ states and (ii) the important energy gap between the low lying emissive doublet states and the more energetic $Cr^{III}(^4T_2)$ excited state in $[Cr^{III}N_6]$ chromophores, which avoids deleterious $Cr^{III}(^2E \rightarrow ^4T_2)$ back intersystem crossing (BISC).

The promising emissive properties of Cr^{III} were early identified in ruby (a $[Cr^{III}O_6]$ chromophore) which displays an impressive red emission at 695 nm with a lifetime around 3.5 ms because the only low energy phonons accessible in solid matrices precludes efficient de-excitation pathways *via* vibration mode coupling. Nevertheless, going from solid to molecules inputs additional high energy ligand vibrations which provides about 500 cm^{-1} of accessible phonons. Those latter, once involved in phonon assisted energy transfers or de-excitations, dramatically shorten the Cr^{III} excited state lifetime of $[Cr^{III}O_6]$ chromophores to 17 μs at 77K in frozen glass and below the microsecond range in solution at room temperature (Table 3) [63]. Therefore, important efforts were provided to identify and to restrict the non-radiative de-excitation pathways in molecular Cr^{III} complexes. BISC was early identified as a significant quenching route, and the shift of the $Cr^{III}(^4T_2)$ level to higher energy thanks to the replacement of O-donors with stronger N-donors was found to be a winning strategy for inducing room temperature emission in molecular complexes. Forster stated that BISC was observed in $Cr^{III}N_{6-x}O_x$ complexes for $x > 3$ [63], while Madge indicated that BISC is predominant when the ^2E-$^4T_2$ energy gap was below 3400 cm^{-1} [115]. Hence, the $Cr^{III}O_6$ chromophores were roughly forsaken [64] and the photophysical studies mainly focused on the $Cr^{III}N_6$ coordination spheres found in homoleptic Cr^{III} complexes (Table 3).

Table 3. Photophysical properties of a selection of homoleptic Cr^{III} complexes.

Complex	τ^{77K} [a] / ms	$\tau^{RT}_{Air\,eq}$ [b] / µs	$\tau^{RT}_{Deaearated}$ [c] / µs	$\Phi^{RT}_{Air\,eq}$ [d] / %	$\Phi^{RT}_{Deaerated}$ [e] / %	Solvent	Refs
$[Cr(H_2O)_6]^{3+}$	0.017					DMSO/H_2O (1/1)	[116]
$[Cr(NH_3)_6]^{3+}$	0.068					DMSO/H_2O (1/1)	[116]
		2.2		0.0055	0.45	H_2O	[16], [115]
$[Cr(D_2O)_6]^{3+}$	0.5					DMSO/H_2O (1/1)	[116]
$[Cr(ND_3)_6]^{3+}$	5.4	3.1				DMSO/H_2O (1/1)-	[116]
$[Cr(CN)_6]^{3-}$	3.95	0.12				DMSO/H_2O (1/1)	[117]
		0.14		0.000005		H_2O	[16]
$[Cr(ox)_3]^{3-}$	1.0					EtOH/H_2O	[63]
$[Cr(en)_3]^{3+}$	0.1					DMSO/H_2O (1/1)	[117]
		1.9		0.0062	0.27	H_2O	[16], [116]
$[Cr(bpy)_3]^{3+}$	5.0	73				DMSO/H_2O (1/1)	[117]
		52	74			H_2O	[55]
		55	63	0.089	0.25	H_2O HCl(1M)	[118]
			290			H_2O HCl(1M) + $HClO_4$ (5M)	[54]
							[54]
$[Cr(phen)_3]^{3+}$	5.3	126				DMSO/H_2O (1/1)	[117]
		37	199			CH_3CN	[119]
		74	356			H_2O	[55]
		71	270		0.43	H_2O HCl(1M)	[55]
			304		1.2	H_2O HCl(1M)	[118]

Table 3. Continued.

$[Cr(Me_4\text{-phen})_3]^{3+}$		27	610			H_2O	[55]
		26	470		0.19	H_2O HCl(1M)	[54]
$[Cr(Me_2\text{-bpy})_3]^{3+}$		77	230			H_2O HCl(1M)	[54]
			196		0.89	H_2O HCl(1M)	[118]
$[Cr(Me_2\text{-phen})_3]^{3+}$	4.3	37	340		0.25	H_2O HCl(1M)	[54]
$[Cr(tpy)_2]^{3+}$	0.54					DMSO/H_2O	[63]
			0.14			H_3CCN	[120]
	0.67				<0.001	CH_3CN/C_2H_5CN (6/4)	[78]
$[Cr(ebzpy)_2]^{3+}$	0.265 (3K)					CH_3CN	[76]
$[Cr(ddpd)_2]^{3+}$		51	899	0.71	12.1	CH_3CN	[51]
		177	898	2.1	11.0	H_2O	
			1164		14.2	D_2O	
	1.3					CH_3CN/C_2H_5CN (6/4)	[78]
$[Cr(D\text{-}ddpd)_2]^{3+}$		190	1200			H_2O	[121]
		170	2100		21.6	D_2O	
$[Cr(tpe)_2]^{3+}$					3.2	H_2O	[113]
			2800		5.4	$H_2O/HClO_4$ (0.1M)	
			4500		8.2	$D_2O/DClO_4$ (0.1M)	
$[Cr(dqp)_2]^{3+}$	3.07					DMSO/H_2O(1/1)	[91]
		83	1270	1.0	5.2	H_2O	

[a] $Cr(^2E)$ excited state lifetime at 77K in frozen matrices. [b] $Cr(^2E)$ excited state lifetime at room temperature in air equilibrated solution. [c] $Cr(^2E)$ excited state lifetime at room temperature in deaerated solution. [d] Experimental quantum yield at room temperature in air equilibrated solution. [e] Experimental quantum yield at room temperature in deaerated solution. Abbreviations: ox = oxalate, en = ethylendiamine, bpy = bipyridine, phen = 1,10-Phénantroline, Me_4-phen = 3,4,7,8-tetramethyl-1,10-phenanthroline, Me_2-bpy = 4,4'-dimethyl-2,2'-bipyridine, Me_2-phen = 4,7-dimethyl-1,10-phenanthroline, tpy = terpyridine, ebzpy = 2,6-bis(1-ethyl-benzimidazol-2-yl)pyridine, ddpd = N,N'-dimethyl-N,N''-dipyridin-2-ylpyridine-2,6-diamine, tpe = 1,1,1-tris(pyrid-2-yl)ethane, dqp = 2,6-di(quinolin-8-yl)pyridine.

The presence of high energy oscillators in the coordination sphere is also incriminated in the shortening of the excited state lifetime and Forster indeed shown that replacing ammonia or water ligands with their deuterated counterparts restores two orders of magnitude longer emission lifetimes at 77K [63]. Harnessing polypyridyl ligands without O-H or N-H bonds in complexes also extended $Cr^{III}(^2E)$ lifetimes to reach several milliseconds at 77K and hundred microsecond at room temperature in degassed solutions. However, the remaining dipolar coupling between the Cr^{III} electric dipole transition moment and the C-H oscillators appeared to be non-negligible since the replacement of hydrogen atoms in phenanthroline or bipyridine ligands with methyl moieties enhances the emission lifetimes by factors 2 and 3, due to the increased distances between the Cr^{III} emissive centre and the C-H oscillators [54,55]. Alternatively, Heinze and coworkers replaced C-H bonds with the low energy oscillating C-D analogues and thus enhanced the $Cr^{III}(^2E)$ lifetimes to reach the millisecond range in room temperature solutions [121].

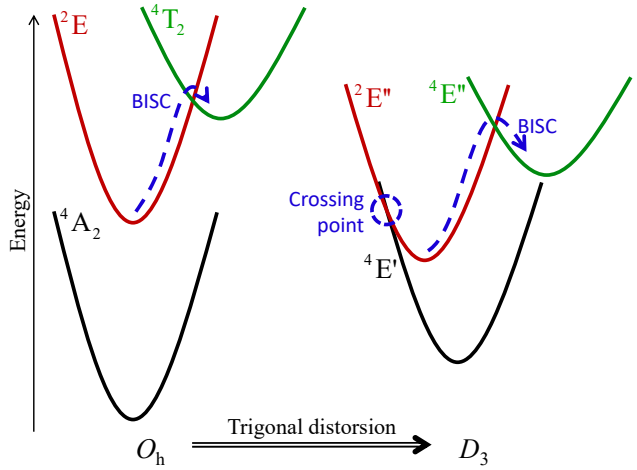

Figure 17. Metal centred excited state of a $Cr^{III}N_6$ complex represented as harmonic potentials for a pure octahedral geometry (O_h) and upon trigonal distortion (D_3), showing the main associated non-radiative de-excitation pathways: back intersystem crossing (BISC), and the low energy crossing point.

The exact geometry of the coordination sphere distortion is also importantly involved and, beyond the weakening effect on the ligand field produced by a trigonal distortion of the $[Cr^{III}N_6]$ chromophore in going from *O* to D_3 symmetry which might favour BISC (Figure 17), the symmetry release of the CrN_6 coordination sphere induces degeneracy breaking of the spectroscopic levels $O(^4A_2) \rightarrow D_3(^4E')$;

$O(^2E) \rightarrow D_3(^2E')$; $O(^2T_1) \rightarrow D_3(^2E' + {}^2A_2)$; $O(^4T_2) \rightarrow D_3(^4E')$ [116,117]. From the shift induced in nuclear coordinates, a low energy crossing point between the low lying anharmonic potentials emerges and provides an accessible efficient non-radiative de-excitation pathway (Figure 17) [14]. Beyond the quenching pathways intrinsically related to the complex structure, some environmental parameters have also dramatic influence on the magnitude of non-radiative rate constant. Energy transfers to O_2 was early highlighted as efficient quenching pathways, justifying the pervasive deareration of solutions. Finally, most of the phonon-assisted non-radiative de-excitation pathways are weakened by temperature decreases so that millisecond range $Cr^{III}(^2E)$ lifetime is recovered for polypyridyl complexes at 77K [54,116]. Appealed by the potential enhancement of the Cr^{III} emitters photophysical features, and inspired by a parent success in Ru^{II} photophysics, Heinze and co-workers designed in 2015 the $[Cr(ddpd)_2]^{3+}$ complex, in which two tridentate fused six-membered chelate rings were bound to Cr^{III}. The resulting strong field and almost undistorted octahedral $Cr^{III}N_6$ chromophore fulfils most of the aforementioned criterions for optimizing the emission properties (Figure 18a) [51,122], a success confirmed four years later with the slightly more rigid $[Cr(dqp)_2]^{3+}$ complex (Figure 18b) [112].

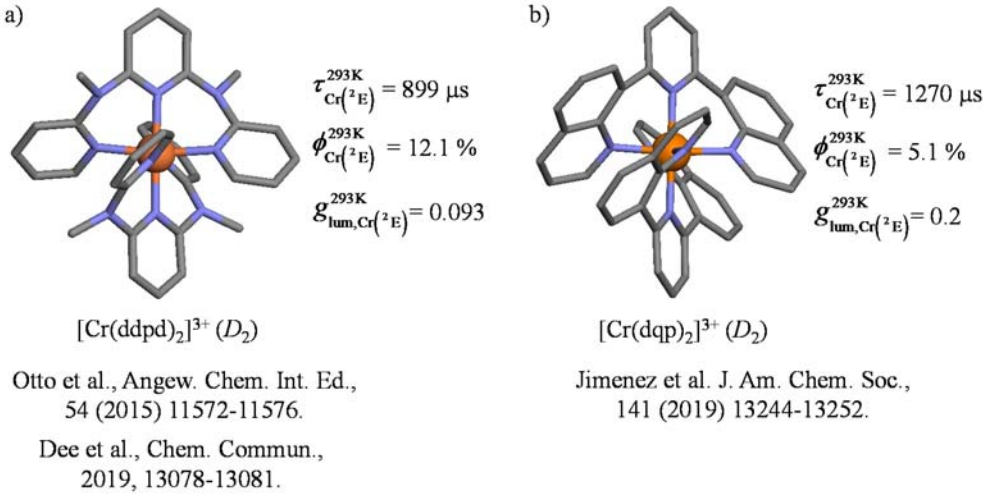

Figure 18. Molecular structures of a) $[Cr(ddpd)_2]^{3+}$ [51,122] and b) $[Cr(dqp)_2]^{3+}$ [112] highlighting the optimized photophysical properties. Color code: C = grey, N = blue, Cr = orange. Associated excited state $Cr(^2E)$ lifetimes, quantum yields (ϕ) and dissymmetry factor (g_{lum}) for circularly polarized luminescence at room temperature are included.

Table 4. Photophysical properties of a selection of heteroleptic Cr^{III} complexes.

Complex	λ_{em} [a] / nm	τ^{10K} [b] / ms	τ^{77K} [c] / ms	$\tau^{RT}_{Air\,eq}$ [d] / μs	$\tau^{RT}_{Deaerated}$ [e] / μs	$\Phi^{RT}_{Air\,eq}$ [f] / %	$\Phi^{RT}_{Deaerated}$ [g] / %	Solvent	Refs
$[Cr(bpy)_3]^{3+}$	730			52	74			H_2O	[55]
$[Cr(bpy)_2(phen)]^{3+}$	730			74	112			H_2O	[55]
$[Cr(bpy)(phen)_2]^{3+}$	730			70	200			H_2O	[55]
$[Cr(phen)_3]^{3+}$	730			74	356			H_2O	[55]
$[Cr(phen)_2(Me_4\text{-}phen)]^{3+}$	734			62	280			H_2O	[55]
$[Cr(phen)(Me_4\text{-}phen)_2]^{3+}$	737			38	450			H_2O	[55]
$[Cr(Me_4\text{-}phen)_3]^{3+}$	739			27	610			H_2O	[55]
$[Cr(bpy)(phen)(Me_4\text{-}phen)]^{3+}$	732			40	154			H_2O	[57]
$[Cr(phen)_2(NH_2\text{-}phen)]^{3+}$	730			0.21	0.21			CH_3CN	[119]
$[Cr(phen)_2(Me_2\text{-}phen)]^{3+}$	730			30	259			CH_3CN	[119]
$[Cr(phen)_2(Ph_2\text{-}phen)]^{3+}$	732			26	317			CH_3CN	[119]
$[Cr(phen)_2(Me_2\text{-}bpy)]^{3+}$	730			31	91			CH_3CN	[119]
$[Cr(phen)_2(Br\text{-}phen)]^{3+}$	730	1.7			214			10K: CH_3CN/C_2H_5CN (6/4) 298K: CH_3CN	[73]

Table 4. Continued.

$[Cr(phen)_2(Alkyn\text{-}phen)]^{3+}$	729	2.9			259			10K: CH_3CN/C_2H_5CN (6/4) 298K: CH_3CN	[73]
$[Cr(phen)_2(NO_2\text{-}phen)]^{3+}$	728	1.4			177			10K: CH_3CN/C_2H_5CN (6/4) 298K: CH_3CN	[73]
$[Cr(phen)_2(dpma)]^{3+}$	747	1.4			23			10K: CH_3CN/C_2H_5CN (6/4) 298K: CH_3CN	[73]
$[Cr(phen)_2(phen\text{-}bzpy)]^{3+}$	726	2.8	3.0	112	32	0.3	0.8	77K: CH_3CN/CH_3NO_2 (6/4) 298K: CH_3CN	[102]
$[Cr(tpy)(ebzpy)]^{3+}$	795	0.264						CH_3CN/C_2H_5CN	[76]
$[Cr(ddpd)(tpy)]^{3+}$	757		1.06	40	1002	0.014	0.06	77K: CH_3CN/C_2H_5CN (6/4) 298K: CH_3CN	[78]
$[Cr(ddpd)(tpy\text{-}COOEt)]^{3+}$	765		1.07	40	980	0.018	0.14	77K: CH_3CN/C_2H_5CN (6/4) 298K: CH_3CN	[78]
$[Cr(dqp)(tpy)]^{3+}$	746		0.7	3.0	578	0.0015	0.2	77K: CH_3CN/C_2H_5CN (6/4) 298K: CH_3CN	[79]
$[Cr(ddpd)(dqp)]^{3+}$	762		1.7	14	642	0.12	6.0	77K: CH_3CN/C_2H_5CN (6/4) 298K: CH_3CN	[79]
$[Cr(dqp)(dqpOMe)]^{3+}$	752		2.7	25	855	0.16	6.5	77K: CH_3CN/C_2H_5CN (6/4) 298K: CH_3CN	[79]

[a] Emission wavelength. [b] $Cr(^2E)$ excited state lifetime at 10K in frozen matrices. [c] $Cr(^2E)$ excited state lifetime at 77K in frozen matrices. [d] $Cr(^2E)$ excited state lifetime at room temperature in air equilibrated solution. [e] $Cr(^2E)$ excited state lifetime at room temperature in deaerated solution. [f] Experimental quantum yield at room temperature in air equilibrated solution. [g] Experimental quantum yield at room temperature in deaerated solution. Abbreviations: bpy = bipyridine, phen = 1,10-Phénantroline, Me_4-phen = 3,4,7,8-tetramethyl-1,10-phenanthroline, Me_2-bpy = 4,4'-dimethyl-2,2'-bipyridine, Me_2-phen = 4,7-dimethyl-1,10-phenanthroline, tpy = terpyridine, ebzpy = 2,6-bis(1-ethyl-benzimidazol-2-yl)pyridine, ddpd = N,N'-dimethyl-N,N''-dipyridin-2-ylpyridine-2,6-diamine, NH_2-phen = 5-amino-1,10-phenanthroline, Ph_2-phen = 4,7-diphenyl-1,10-phenanthroline, Br-phen = 5-bromo-1,10-phenanthroline, Alkyn-phen = 5-Ethynyl-1,10-phenanthroline, NO_2-phen = 5-nitro-1,10-phenanthroline, dpma = di(pyrid-2-yl)(methyl)amine, phen-bzpy = 2,6-bis(N-methyl-benzimidazol-2-yl)-4-((1,10-phenanthrolin-5-yl)ethynyl)pyridine), tpy-COOEt = 4'-carbethoxy-2,2':6',2"-terpyridine.

The photophysics of heteroleptic complexes does not significantly differs from that of their homoleptic analogues as long as the $[Cr^{III}N_6]$ coordination sphere is not modified (Figures 6, 8-10 and Table 4). However, sequential substitution of ligands in tri-didentate complexes $[Cr(N^{\frown}N)_n(N'^{\frown}N')_{3-n}]^{3+}$ (n = 0, 1, 2, 3) provides heteroleptic complexes (n = 1, 2) with intermediate photophysical properties surrounded by those of the parents homoleptic complexes (n = 0, 3). For instance, the series of heteroleptic complexes $[Cr(bpy)_n(phen)_{3-n}]^{3+}$ (Table 4, entries 1-4) or $[Cr(phen)_n(Me_4\text{-}phen)_{3-n}]^{3+}$ (Table 4, entries 4-7) allows the fine tuning of the excited state lifetime upon the introduction of new ligands with no change in the symmetry of the $[Cr^{III}N_6]$ chromophore [55]. However, the lower C_2 symmetry point group of heteroleptic $[Cr(N^{\frown}N)_n(N'^{\frown}N')_{3-n}]^{3+}$ complexes, compared with D_3 symmetry found for their homoleptic $[Cr(N^{\frown}N)_3]^{3+}$ analogue, results in a modification of the complexes emission with the systematic splitting of the absorption and emission bands [49]. Prompted by the attractive photophysical properties of homoleptic di-tridentate complexes holding six membered chelate rings ($[Cr(ddpd)_2]^{3+}$ and $[Cr(dqp)_2]^{3+}$) depicted in Figure 17, Jiménez et al. prepared novel series of heteroleptic complexes characterized by the $[Cr(N^{\frown}N^{\frown}N)(N'^{\frown}N'^{\frown}N')]^{3+}$ formula containing at least one ddpd or one dqp unit (Figures 9-10 and Table 4, entries 18-23) [78-79]. In $[Cr(ddpd)(tpy)]^{3+}$, $[Cr(ddpd)(tpy\text{-}COOEt)]^{3+}$ and $[Cr(dqp)(tpy)]^{3+}$, the energy of the emission bands are in line with intermediate properties regarding the parent homoleptic complexes. In addition the presence of one six-membered ddpd or dqp ligand is sufficient to provide an emission lifetime within the millisecond range in deaerated room temperature solutions, but the corresponding quantum yields suffer from the presence of the bound five-membered chelates in tpy ligand. However, the synthetic possibilities offered by the functionalization of tpy unit opens important perspectives for the introduction of long-lived $[Cr^{III}N_6]$ chromophores into polymetallic architectures *via* a rational complex-as-ligand approach. For instance, the carboxylate group of the complex $[Cr(ddpd)(tpy\text{-}COOEt)]^{3+}$ can be directly harnessed for this purpose. Interestingly, the presence of a free binding unit does not affect the complexes photophysical properties, an observation confirmed by studies conducted on the tri-didentate building block $[Cr(phen)_2(phen\text{-}bzpy)]^{3+}$ [102].

Pushing further the latter synthetic method results in the isolation of heteroleptic Cr^{III} complexes $[Cr(ddpd)(dqp)]^{3+}$ and $[Cr(dqp)(dqp\text{-}OMe)]^{3+}$ with two different tridentate fused (6-6)-membered chelate rings (Figure 11). The favourable structural and electronic properties of the latter systems lead to long excited states lifetimes (>600 μs) and high quantum yields (>5%), which make these chromium complexes as sustainable alternative to expensive precious metal-based complexes, for their insertion into heterometallic supramolecular architectures within the frame of energy-conversion technologies.

The use of heteroleptic Cr^{III} complexes for the construction of multimetallic luminescent materials remains quite underexplored so far. The remarkable work of Kazaiki and co-workers on $[(acac)_2Cr(ox)]$- and more recently of Doistau et al. on $[Cr(phen)_2(phen\text{-}bzpy)]^{3+}$ et al. are at the cutting-edge in this field. In the first case, Kazaiki and co-workers used the oxalate bridge to ensure efficient Cr ↔ Ln energy transfer processes and a series of Cr-Ln with tuneable emission properties was prepared and characterized by these authors (Figure 14a). When introducing lanthanide acceptors possessing low-energy emissive levels (Ln = Nd, Ho, Er, Tm, Yb), the Cr → Ln energy transfer was followed by Ln-centred NIR luminescence [65,95-99]. At room temperature, the Cr-Ln energy transfer dominates and only the Ln centred emission could be detected. At low temperature, dual emission arising from Cr^{III} centred and Ln^{III} centred luminescence resulted from a competition between energy transfer and Cr^{III} emission. Upon introducing Eu^{III} or Tb^{III}, the Cr^{III} luminescence is partially quenched, whereas Ln centred emission is absent. With closed-shell Ln^{III}, the Cr centred luminescence is not disrupted except for a minor increase of the nephelauxetic effect in going from La to Lu (600 cm^{-1} blue shifted of Cr-centred emission). Alternatively, the $[Cr(phen)_2(phen\text{-}bzpy)]^{3+}$ complex (noted below as $[CrL]^{3+}$) has been used for the preparation of the trinuclear $[CrLZn^{II}LCr]^{8+}$ and $[CrLFe^{II}LCr]^{8+}$ adducts (Figure 15). The long $Cr(^2E)$ excited state lifetime measured for $[CrL]^{3+}$ in frozen acetonitrile (2.8(3) ms) is slightly enhanced for $[CrLZn^{II}LCr]^{8+}$ (3.2(2) ms) and $[CrLZn^{II}]^{5+}$ (3.8(2) ms, Table 2). However, vibrations associated with the central [Zn(bis-benzimidazolepyridine)$_2$] unit limit the room-temperature $Cr(^2E)$ excited state lifetimes to 43(2) μs,

a value considerably shorter than that found for the precursor $[CrL]^{3+}$ (112(8) μs). The introduction of Fe^{II} as an acceptor in $[CrLFe^{II}LCr]^{8+}$ induces the complete quenching of the chromium-centred emission in the whole temperature range (10-293 K). Interestingly, a quantitative intramolecular $Cr(^2E) \rightarrow Fe^{II}$ energy transfer occurs in this complex despite the long intermetallic Cr···Fe distance (ca. 13.9 Å) and the weak spectral overlap between the emission spectrum of the Cr^{III} donor and the absorption spectrum of the Fe^{II} acceptor. The authors concluded that the alkyne bridges are likely efficient for promoting intermetallic electronic communication via a double electron exchange mechanism [102].

6. Conclusions and perspectives

Trivalent chromium, Cr^{III}, shares with Ru^{II} the advantages of being open-shell metallic centres with appealing photophysical and photochemical properties when they exist as pseudo-octahedral $[MN_6]^{n+}$ chromophores. Moreover, their kinetic inertness toward ligand exchange processes makes them compatible with the preparation of tuneable heteroleptic complexes. However, Cr^{III} is much harder than Ru^{II} according to *Pearson*'s classification [62], and the preparation of $[Cr^{III}N_6]$ units with soft nitrogen donors is more challenging. On the other side, the much larger abundance of chromium in the earth crust justifies the efforts made to introduce trivalent chromium in extended light-converting devices. Inspired by the intense synthetic activities focused on ruthenium chemistry during the last four decades, the selective and successful preparation of primary heteroleptic building blocks of $[CrN_{(6-n)}X_n]^{(3-n)+}$ indeed exploited the relative strengths of the M-X (X = halide, pseudo-halides or solvent molecules) and M-N bonds, which can be further modulated by the chelate effect inherent to didentate N^N or tridentate N^N^N ligands. With this in mind, the accessible heteroleptic *cis*/*trans*-$[Cr(N^N)_2X_2]^+$ and *fac*/*mer*-$[Cr(N^N^N)X_3]$ complexes, with X = halide or cyanide, represents remarkable building blocks for further construction of larger polynuclear/polymetallic edifices as demonstrated by Long and co-workers with the rational design of polymetallic cubic assemblies using *fac*-$[(Me_3tacn)Cr(CN)_3]$ basic units (Figure 13b). Subsequently, the latter complex-as-ligand strategy has been applied for the preparation of various target heteroleptic $[Cr^{III}N_6]$ chromophores, among

which the mononuclear $[Cr(N^{\frown}N)_2(N'^{\frown}N')]^{3+}$ (Figure 6) and $[Cr(N^{\frown}N^{\frown}N)(N'^{\frown}N'^{\frown}N')]^{3+}$ (Figures 8-10) complexes are currently the most studied systems. To the best of our knowledge, the extension of this synthetic strategy toward discrete polynuclear assemblies based on the target $[Cr^{III}N_6]$ unit, as it is common for related $[Ru^{II}N_6]$ units in sophisticated 2D and 3D aggregates [109,110], is still in its infancy and has been only applied for the preparation of dinuclear (Figure 9) and trinuclear (Figure 15) rod-like complexes. There is however no obvious reason preventing the design of a rich library of Cr^{III}-containing complex-as-ligands inspired by the $[Cr(phen)_2(phen\text{-}bzpy)]^{3+}$ unit (Figure 15). It is worth stressing here that the triply charged $[Cr^{III}N_6]$ chromophores, compared to doubly charged $[Ru^{II}N_6]$ analogues, induces a minimum $3^2/2^2 = 2.25$ larger repulsive electrostatic energetic interaction (the *Born* equation predicts a z^2/R dependence) when using $[Cr^{III}N_6]$ building block (Figure 14). The stability of larger edifices will be therefore limited with trivalent chromium and the design of negatively charged free binding unit in complex-as-ligand units should be preferred. An alternative strategy, previously developed for similar limitations encountered with Ir^{III} complexes, consists in the binding of negatively charged N-carbene ligands to reduce the metallic charge [123]. There is no doubt that the limited exploration and accessibility of heteroleptic $[Cr^{III}N_6]$ building blocks represents a major handicap for their incorporation into extended assemblies displaying intermetallic communications and working as light-conversion devices. Homoleptic analogues programmed in triple-stranded CrErCr helicates were at the origin of the first reported molecular light-upconversion phenomenon [45] and we do believe that heteroleptic $[Cr^{III}N_6]$ chromophores have the potential to open novel perspectives for introducing cheap metals into sophisticated devices.

7. References

[1] N. Eastaugh, V. Walsh, T. Chaplin, R. Siddall, Pigment Compendium - A Dictionary of Historical Pigments, first ed., Elsevier Butterworth-Heinemann, Oxford, 2004. https://doi.org/10.4324/9780080473765.

[2] L. R. Nelson, The preparation of chromium metal by a sealed, cold-hearth, plasma assisted aluminothermic method, J. South African Institute of Mining and Metallurgy, 1996, 135-144.

[3] National Research Council, High-Purity Chromium Metal: Supply Issues for Gas-Turbine Superalloys, The National Academies Press, 1995. https://doi.org/10.17226/9248.

[4]. E.A. Brandes, H.T. Greenaway, H.E.N. Stone, Ductility in Chromium, Nature 178 (1956) 587. https://doi.org/10.1038/178587a0.

[5] R.J. Gettens, Chrome yellow. Painting Materials: A Short Encyclopaedia. Courier Dover Publications. (1966) 105–106. ISBN 978-0-486-21597-6.

[6] C.E. Housecroft, A.G. Sharpe, Inorganic Chemistry, Second Ed., Pearson, Harlow, Essex, England, 2005.

[7] T.H. Maiman, Stimulated Optical Radiation in Ruby, Nature 187 (1960) 493-494. https://doi.org/10.1038/187493a0.

[8] L. S. Forster, The Photophysics of chromium(III) Complexes. Chem. Rev. 90 (1990) 331-353. https://doi.org/10.1021/cr00100a001.

[9] N.A.P. Kane-Maguire, Photochemistry and photophysics of coordination compounds: chromium Top Curr. Chem. 280 (2007) 37-67. https://doi.org/10.1007/128_2007_141

[10] A. Hauser, C. Reber, Spectroscopy and chemical bonding in transition metal complexes Structure and Bond. 172 (2017) 291-312. https://doi.org/10.1007/430_2015_195.

[11] O.S. Wenger, Photoactive Complexes with Earth-Abundant Metals, J. Am. Chem. Soc. 140 (2018) 13522-13533. https://doi.org/10.1021/jacs.8b08822.

[12] C. Forster, K. Heinze, Photophysics and photochemistry with Earth-abundant metals – fundamentals and concepts, Chem. Soc. Rev. 49 (2020) 1057-1070. https://doi.org/10.1039/C9CS00573K.

[13]. A. Büldt, O.S. Wenger, Chromium complexes for luminescence, solar cells, photoredox catalysis, upconversion, and phototriggered NO release, Chem. Sci. 8 (2017) 7359-7367. https://doi.org/10.1039/C7SC03372A.

[14] S. Otto, M. Dorn, C. Förster, M. Bauer, M. Seitz, K. Heinze, Understanding and exploiting long-lived near-infrared emission of a molecular ruby, Coord. Chem. Rev. 359 (2018) 102-111. https://doi.org/10.1016/j.ccr.2018.01.004.

[15] A. D. Kirk, G. B. Porter, Luminescence of Chromium^{III} complexes. J. Phys. Chem. 84 (1980) 887-891. https://doi.org/10.1021/j100445a020.

[16] A. D. Kirk, Photochemistry and photophysics of chromium(III) complexes, Chem. Rev. 99 (1999) 1607-1640. https://doi.org/10.1021/cr960111+.

[17] A. D. Kirk, C. Namasivayam, Synthesis of chromium Cr(tacn)X_3 compounds (tacn = 1,4,7-triazacyclononane). Photochemistry and emission properties of the triisothiocyanate, Inor. Chem. 27 (1988) 1095-1099. https://doi.org/10.1021/ic00279a032

[18] J.F. Endicott, T. Ramasami, R. Tamilarasan, R.B. Lessard, C.K. Ryu, G. Brubaker, Structure and reactivity of the metal-centered transition metal excited states, Coord. Chem. Rev. 77 (1987) 1-87. https://doi.org/10.1016/0010-8545(87)85032-4.

[19] P. A. Scattergood, Recent advances in chromium coordination chemistry: luminescent materials and photocatalysis, Organometallic Chemistry, 43 (2020) 1-34. DOI: 10.1039/9781788017077-00001

[20] K. F. Purcell and J. F. Kotz. Inorganic Chemistry, W.B. Saunders Company, Philadelphia, USA, 1977.

[21] S. F. A. Kettle, Physical Inorganic Chemistry, A coordination Chemistry Approach, Oxford University Press, 1996.

[22] E.C. Constable, C.E. Housecroft, Coordination chemistry: the scientific legacy of Alfred Werner, Chem. Soc. Rev. 42 (2013) 1429-1439. https://doi.org/10.1039/C2CS35428D

[23] L. Helm, A.E. Merbach, Inorganic and Bioinorganic Solvent Exchange Mechanisms
Chem. Rev. 105 (2005) 1923-1959. https://doi.org/10.1021/cr030726o.

[24] D.T. Richens, Ligand Substitution Reactions at Inorganic Centers, Chem. Rev. 105 (2005) 1961-2002. https://doi.org/10.1021/cr030705u.

[25] M. L. Tobe, Inorganic reactions mechanisms, Thomas Nelson and Sons, London, 1972

[26] C. H. Langford and H. B. Gray, Ligand substitution processes, W. A. Benjamin Inc., 1965

[27] R. G. Pearson and P. C. Ellgen, Mechanism of inorganic reactions in solution, Physical Chemistry, an advance treatise, volume VII, H. Eyring, ed., Academic Press, New York, 1975

[28] L. Cattalini, The intimate mechanism of replacement in d^8 square-planar complexes, Prog. Inorg. Chem. 13 (1970) 263-327. https://doi.org/10.1002/9780470166147.ch6.

[29] B.J. Coe, S.J. Glenwright, Trans-effects in octahedral transition metal complexes, Coord. Chem. Rev. 203 (2000) 5-80. https://doi.org/10.1016/S0010-8545(99)00184-8.

[30] F. Basolo and R. G. Pearson, Mechanisms of inorganic reactions, 2nd edition, John Wiley and Sons, New York, 1967

[31] R .G. Wilkins, the study of kinetics and mechanism of reactions of transition metal complexes, Allyn and Bacon, Inc., Boston, 1974

[32] A. Peloso, Kinetics of nickel, palladium and platinum complexes, Coord. Chem, Rev. 10 (1973) 123-181. https://doi.org/10.1016/S0010-8545(00)80233-7

[33] G. Schreckenbach, Differential Solvation**,** Chem. Eur. J. 23 (2017) 3797-3803. https://doi.org/10.1002/chem.201604075.

[34] J. Ribas Gispert, Coordination Chemistry, Wiley-VCH Verlag, Weinheim, 2008.

[35] B. N. Figgis, M. Hitchman, Ligand Field Theory and Its Applications, Wiley-VCH, New York, Chichester, Weinheim, Brisbane, Singapore, Toronto, 2000.

[36] M. L. Tobe, Base hydrolysis of octahedral complexes, Acc. Chem. Res. 3 (1970) 377–385. https://doi.org/10.1021/ar50035a003

[37] H. Marai, E. Kita, J. Wiśniewska, Kinetics and mechanism of base hydrolysis of mer-[Cr(pic)3] 0 and [Cr(ox)2(pic)]2- (pic = picolinate, ox = oxalate), Transit. Met. Chem. 37 (2012) 55–62. https://doi.org/10.1007/s11243-011-9556-1.

[38] E. Kita, K. Gołembiewska, Kinetics and mechanism of tris-quinolinatochromium(III) aquation in $HClO_4$ media, Transit. Met. Chem. 32 (2007) 56-63 https://doi.org/10.1007/s11243-006-0128-8

[39] E. Kita H. Marai, K Zaja¸ Synthesis and kinetic studies in aqueous solution on chromium(III) complexes with isocinchomeronic acid—potential new biochromium sources, Transit. Met. Chem. 33 (2008) 211-217 https://doi.org/10.1007/s11243-007-9025-z

[42] E. Kita, H. Marai, Kinetics and mechanism of base hydrolysis of chromium(III) complexes with oxalates and quinolinic acid, Transit. Met. Chem. 34 (2009) 585-591 https://doi.org/10.1007/s11243-009-9234-8

[43] E. Kita, H. Marai, L. Michał, M. Jasiński, T. Drewa, Mixed-ligand chromium(III)-oxalate-pirydinedicarboxylate complexes: Potential biochromium sources: Kinetic studies in NaOH solutions and effect on 3T3 fibroblasts proliferation, Transit. Met. Chem. 35 (2010) 177–184. https://doi.org/10.1007/s11243-009-9311-z.

[44] E. Kita, H. Marai, Ł. Iglewski, Chromium(III) complexes with lutidinic acid: Kinetic studies in $HClO_4$ and NaOH solutions, Transit. Met. Chem. 34 (2009) 75–84. https://doi.org/10.1007/s11243-008-9160-1

[45] M. Maestri, F. Bolletta, N. Serpone, L. Moggi, V. Balzani, Kinetics of ligand substitution of tris(2,2'-bipyridine)chromium(III) in aqueous solutions, Inorg. Chem. 15 (1976) 2048–2051. https://doi.org/10.1021/ic50163a007

[46] M.A. Jamieson, N. Serpone, M.S. Henry, M.Z. Hoffman, Temperature dependence of the photoaquation of tris(2,2'-bipyridine)chromium(III) ion in alkaline solution Inorg. Chem. 18 (1979) 214–216. https://doi.org/10.1021/ic50191a048

[47] E.C. Constable, C.E. Housecroft, M. Neuburger, J. Schönle, J.A. Zampese, The surprising lability of bis(2,2':6',2"-terpyridine)-chromium(III) complexes, Dalton Trans. 43 (2014) 7227-7235. https://doi.org/10.1039/C4DT00200H.

[48] C.C. Scarborough, K.M. Lancaster, S. DeBeer, T. Weyhermüller, S. Sproules, K. Wieghardt, Experimental Fingerprints for Redox-Active Terpyridine in $[Cr(tpy)_2](PF_6)_n$ (n = 3–0), and the

Remarkable Electronic Structure of $[Cr(tpy)_2]^{1-}$, Inorg. Chem. 51 (2012) 3718–3732. https://doi.org/10.1021/ic2027219

[49] C.C. Scarborough, S. Sproules, T. Weyhermüller, S. DeBeer, K. Wieghardt, Electronic and Molecular Structures of the Members of the Electron Transfer Series $[Cr(tbpy)_3]^n$ (n = 3+, 2+, 1+, 0): An X-ray Absorption Spectroscopic and Density Functional Theoretical Study Inorg. Chem. 50 (2011) 12446–12462. https://doi.org/10.1021/ic201123x

[50] P.S. Wagenknecht, P.C. Ford, Metal centered ligand field excited states: their role in the design and performance of transition metal based photochemical molecular devices, Coord. Chem. Rev. 255 (2011) 591-616. https://doi.org/10.1016/j.ccr.2010.11.016.

[51] S. Otto, M. Grabolle, C. Förster, C. Kreitner, U. Resch-Genger, K. Heinze, [Cr(ddpd)2]3+: A molecular, water-soluble, highly NIR-emisssive Ruby analogue, Angew. Chem. Int. Ed. 54 (2015) 11572-11576. https://doi.org/10.1002/anie.201504894.

[52] G.A. Lawrance, Leaving Groups on Inert Metal Complexes with Inherent or Induced Lability, Adv. Inorg. Chem. 34 (1986) 145-194. https://doi.org/10.1016/S0898-8838(08)60016-1.

[53] G. A. Lawrance, Coordinated Trifluoromethanesulfonate and Fluorosulfate, Chem. Rev. 86 (1986) 17-33. https://doi.org/10.1021/cr00071a002

[54] N. Serpone, M.A. Jamieson, M.S. Henry, M.Z. Hoffman, F.M. Bolletta, M. Maestri, Excited-state behavior of polypyridyl complexes of chromium(III), J. Am. Chem. Soc. 101 (1979) 2907-2916. https://doi.org/10.1021/ja00505a019.

[55] K.D. Barker, K.A. Barnett, S.M. Connel, J.W. Glaeser, A.J. Wallace, J. Wildsmith, B.J. Herbert, J.F. Wheeler, N.A.P. Kane-Maguire, Synthesis and characterization of heteroleptic $[Cr(diimine)_3]^{3+}$ complexes, Inorg. Chim. Acta 316 (2001) 41-49. https://doi.org/10.1016/S0020-1693(01)00377-2.

[56] H. Taube, A. Scott, Complexing tendency of trifluoromethylsulfonate ion as measured using chromium(III), Inorg. Chem. 10 (1971) 62-66. https://doi.org/10.1021/ic50095a013.

[57] E.G. Donnay, J.P. Schaeper, R.D. Brooksbank, J.L. Fox, R.G. Potts, R.M. Davidsdon, J.F. Wheeler, N.A.P. Kane-Maguire, Synthesis and characterization of tris(heteroleptic) diimine

complexes of chromium(III), Inorg. Chim. Acta 360 (2007) 3272-3280. https://doi.org/10.1016/j.ica.2007.03.055.

[58] E.C. Constable, C.E. Housecroft, M. Neuburger, J. Schönle, J.A. Zampese, The surprising lability of bis(2,2':6',2"-terpyridine)-chromium(III) complexes, Dalton Trans. 43 (2014) 7227-7235. https://doi.org/10.1039/C4DT00200H.

[59] C. Garcia, G. Ferraudi, A.G. Lappin, M. Isaacs, Synthesis, spectral, electrochemical and flash photolysis studies of Fe(II), Ni(II) tetrapyridylporphyrins coordinated at the periphery with chromium(III) phenanthroline complexes. Inorg. Chim. Acta 386, (2012), 73-82. https://doi.org/10.1016/j.ica.2012.02.023

[60] A. Reinecke, Über Rhodanchromammonium-Verbindungen, Liebigs. Ann. Chem. 126 (1863) 113-118. https://doi.org/10.1002/jlac.18631260116.

[61] N. Costăchescu, Fluorures Complexes de Chrome, Ann. Sci. Univ. Jassy, 7 (1912) 87-100. https://doi.org/10.1039/C19680000038.

[62] D.M.P. Mingos, 50 Years of Structure and Bonding – The Anniversary Volume Structure and Bond 172 (2016) 1-18.

[63] L.S. Forster, The Photophysics of Chromium(III) Complexes, Coord. Chem. Rev. 227 (2002) 59-92, https://doi.org/10.1021/cr00100a001.

[64] A.A.A. Al-Riyahee, P.N. Horton, S.J. Coles, A.J. Amoroso, S.J. Pope, Syntheses, X-ray structures and characterisation of luminescent chromium(III) complexes incorporating 8-quinolinato ligands, Polyhedron 157 (2018) 396-405. https://doi.org/10.1016/j.poly.2018.10.019.

[65] T. Sanada, T. Suzuki, T. Yoshida, S. Kaizaki, Heterodinuclear Complexes Containing d- and f-block Elements: Synthesis, Structural Characterization, and Metal-Metal Interactions of Novel Chromium(III)-Lanthanide(III) Compounds Bridged by Oxalate, Inorg. Chem. 37 (1998) 4712;

[66] L. Aboshyan-Sorgho, M. Cantuel, S. Petoud, A. Hauser, C. Piguet, Optical sensitization and upconversion in discrete polynuclear chromium-lanthanide complexes, Coord. Chem. Rev. 256 (2012) 1644-1663. https://doi.org/10.1016/j.ccr.2011.12.013.

[67] N. Fahmi, S. Shrivastava, R. Meena, S.C. Joshi, R.V. Singh, Microwave assisted synthesis, spectroscopic characterization and biological aspects of some new chromium(III) complexes derived from N^O donor Schiff bases, New J. Chem. 37 (2013) 1445-1453. https://doi.org/10.1039/C3NJ40907D.

[68] C. Pichon, B. Elrez, V. Bereau, C. Duhayon, J.P. Sutter, From Heptacoordinated Cr-III Complexes with Cyanide or Isothiocyanate Apical Groups to 1D Heterometallic Assemblages with All-Pentagonal-Bipyramid Coordination Geometries, Eur. J. Inorg. Chem., (2018) 340-348. https://doi.org/10.1002/ejic.201700845.

[69] Pichon, N. Suaud, C. Duhayon, N. Guihery, J.P. Sutter, Cyano-Bridged Fe(II)-Cr(III) Single-Chain Magnet Based on Pentagonal Bipyramid Units: On the Added Value of Aligned Axial Anisotropy, J. Am. Chem. Soc., 140 (2018) 7698-7704. https://doi.org/10.1021/jacs.8b03891.

[70] K. Wieghardt, I. Tolksdorf, W. Herrmann, Coordination chemistry of the bimacrocyclic, potentially binucleating ligand 1,2-bis(1,4,7-triaza-1-cyclononyl)ethane (dtne). Electrochemistry of its first transition series metal(II,III) complexes. Characterization of the new hemerythrin model complex $[Fe_2(dtne)(\mu\text{-}O)(\mu\text{-}CH_3CO_2)_2]Br_2\cdot H_2O$, Inorg. Chem. 24 (1985) 1230-1235. https://doi.org/10.1021/ic00202a024.

[71] D. A. House, D. Yang, Chromium(III) complexes of the linear tetraamine 1,4,8,11-tetraazaundecane (entnen). Synthesis, configurational assignments, optical activity and hydrolysis kinetics, Inorg. Chim. Acta 74 (1983) 179-189. https://doi.org/10.1016/S0020-1693(00)81425-5.

[72] J. Glerup, J. Josephsen, K. Michelsen, E. Pedersen, C.E. Schäffer, Preparation of Chromium(III) Complexes with Two Fluorine Atoms and Four Nitrogen Atoms as Ligators. trans-Difluorotetrakis(pyridine)chromium(III) Salts as Initial Materials, Acta. Chem. Scand., 24 (1970) 247-254. http://doi.org/10.3891/acta.chem.scand.24-0247.

[73] B. Doistau, G. Collet, E.A. Bolomey, V. Sadat-Noorbakhsh, C. Besnard, C. Piguet, Heteroleptic Ter-Biendentate Cr(III) Complexes as Tunable Optical Sensitizers, Inorg. Chem. 57 (2018) 14362-14373. https://doi.org/10.1021/acs.inorgchem.8b02530.

[74] J. Schönle, E.C. Constable, C.E. Housecroft, M. Neuburger, J.A. Zampese, Heteroleptic chromium(III) tris(diimine) [Cr(N^N)2(N′^N′)]3 + complexes, Inorg. Chem. Commun. 51 (2015) 75-77. https://doi.org/10.1016/j.inoche.2014.11.012.

[75] J. Schönle, E.C. Constable, C.E. Housecroft, A. Prescimone, J.A. Zampese, Homoleptic and heteroleptic complexes of chromium(III) containing 4′-diphenylamino-2,2′:6′,2″-terpyridine ligands**,** Polyhedron 89 (2015) 182-188. https://doi.org/10.1016/j.poly.2015.01.015.

[76] D. Zare, B. Doistau, H. Nozary, C. Besnard, L. Guénée, Y. Suffren, A.-L. Pelé, A. Hauser, C. Piguet, Cr(III) as an alternative to Ru(II) in metallo-supramolecular chemistry, Dalton Trans. 46 (2017) 8992–9009. https://doi.org/10.1039/C7DT01747B.

[77] W. Kharmawphlang, S. Choudhury, A.K. Deb, S. Goswami, Convenient Approach to the Direct Syntheses of Chromium Complexes from Chromium(III) Chloride, Inorg. Chem. 34 (1995) 3826-3828. https://doi.org/10.1021/ic00118a035.

[78] J.-R. Jiménez, B. Doistau, C. Besnard, C. Piguet, Versatile Heteroleptic Bis-Terdentate Cr(III) Chromophores Displaying Room Temperature Millisecond Excited State Lifetimes, Chem. Commun. 54 (2018) 13228-13231. https://doi.org/10.1039/C8CC07671E.

[79] J.-R. Jiménez, M. Poncet, B. Doistau, C. Besnard, C. Piguet, Luminescent polypyridyl heteroleptic CrIII complexes with high quantum yields and long excited state lifetimes, Dalton Trans. 49 (2020) 13528-13532. https://doi.org/10.1039/D0DT02872J.

[80] E.J.L. McInnes, G.A. Timco, G.F.S. Whitehead, R.E.P. Winpenny, Heterometallic Rings: Their Physics and use as Supramolecular Building Blocks, Angew. Chem. Int. Ed. 54 (2015) 14244-14269. https://doi.org/10.1002/anie.201502730.

[81] Y. Suffren, B. Golesorkhi, D. Zare, L. Guénée, H. Nozary, S.V. Eliseeva, S. Petoud, A. Hauser, C. Piguet, Taming Lanthanide-Centered Upconversion at the Molecular Level, Inorg. Chem. 55 (2016) 9964-9972. https://doi.org/10.1021/acs.inorgchem.6b00700.

[82] T. Birk, K.S. Pedersen, C.A. Thuesen, T. Weyhermueller, M. Scha-Magnusen, S. Piligkos, H. Weihe, S. Mossin, M. Evangelisti, J. Bendix, Fluoride bridges as structure-directing motifs in 3d-4f cluster chemistry, Inorg. Chem. 51 (2012) 5435-5443. https://doi.org/10.1021/ic300421x.

[83] J. Dreiser, K.S. Pedersen, C. Piamonteze, S. Rusponi, Z. Salman, M. Ali, E., M. Schau-Magnussen, C.A. Thuese, S. Piligkos, H. Weihe, H. Mutka, O. Waldmann, P. Oppeneer, J. Bendix, F. Nolting, H. Brune, Direct observation of a ferri-to-ferromagnetic transition in a fluoride-bridged 3d-4f molecular cluster, Chem. Sci. 3 (2012) 1024-1032. https://doi.org/10.1039/C2SC00794K.

[84] Y. Guo, G.-F. Xu, C. Wang, T.-T. Cao, J. Tang, Z.-Q. Liu, Y. Ma, S.-P. Yan, P. Cheng, D.-Z. Liao, Cyano-bridged terbium(III)-chromium(III) bimetallic quasi-one-dimensional assembly exhibiting long-range magnetic ordering, Dalton Trans. 41 (2012) 1624-1629. https://doi.org/10.1039/C1DT11655J.

[85] T. Shiga, A. Mishima, K. Sugimoto, H. Okawa, H. Oshio, M. Ohba, One-dimensional 3d-3d-4f trimetallic assemblies consisting of Cu(II)2Ln(III) trinuclear complexes and hexacyanometallate, Eur. J. Inorg. Chem. (2012) 2784-2791. https://doi.org/10.1002/ejic.201101060.

[86] C.A. Thuesen, K.S. Pedersen, M. Schau-Magnussen, M. Evangelisti, J. Vibenholt, S. Piligkos, H. Weihe, J. Bendix, Fluoride-bridged {Ln2Cr2} polynuclear complexes from semi-labile mer-[CrF3(py)3] and [Ln(hfac)3(H2O)2], Dalton Trans. 41 (2012) 11284-11292. https://doi.org/10.1039/C2DT31302B.

[87] M. Holynska, M. Korabik, Preparation and properties of a series of [Cr2Ln2] oximato-bridged complexes, Eur. J. Inorg. Chem. (2013) 5469-5475. https://doi.org/10.1002/ejic.201300658.

[88] S.K. Langley, D.P. Wielechowski, B. Moubaraki, K.S. Murray, Enhancing the magnetic blocking temperature and magnetic coercity of {Cr(III)2Ln(III)2} single-molecule magnets via bridging ligand modification, Chem. Commun. 52 (2016) 10976-10979, https://doi.org/10.1039/C6CC06152D.

[89] H. Han, X. Li, X. Zhu, G. Zhang, S. Wang, X. Hang, J. Tang, W. Liao, Single-molecule-magnet behavior in a calix[8]arene-capped {Tb6(UUU)Cr(III)} cluster, Eur. J. Inorg. Chem. (2017) 2088-2093. https://doi.org/10.1002/ejic.201700013.

[90] C. Cui, J.-P. Cao, X.-M. Luo, Q.-F. Lin, Y. Xu, Two Pairs of Chiral "Tower-Like" Ln4Cr4 (Ln = Gd, Dy) Clusters: Syntheses, Structure, and Magneticaloric Effect, Chem. Eur. J. 24 (2018) 15295-15302. https://doi.org/10.1002/chem.201802804.

[91] R. Lescouëzec, L.M. Toma, J. Vaissermann, M. Verdaguer, F.S. Delgado, C. Ruiz-Pérez, F. Lloret, M. Julve, Design of single chain magnets through cyanide-bearing six-coordinate complexes, Coord. Chem. Rev. 249 (2005) 2691-2729. https://doi.org/10.1016/j.ccr.2005.09.017.

[92] L. Toma, R. Lescouezec, J. Vaissermann, F.S. Delgado, C. Ruiz-Perez, R. Carrasco, J. Cano, F. Lloret, M. Julve, Nuclearity Controlled Cyanide-Bridged Bimetallic CrIII–MnII Compounds: Synthesis, Crystal Structures, Magnetic Properties and Theoretical Calculations, Chem. Eur. J. 10 (2004) 6130-6145. https://doi.org/10.1002/chem.200400611.

[93] P.A. Berseth, J.J. Sokol, M.P. Shores, J.L. Heinrich, J.R. Long, High-Nuclearity Metal-Cyanide Clusters: Assembly of a Cr8Ni6(CN)24 Cage with a Face-Centered Cubic Geometry, J. Am. Chem. Soc. 122 (2000) 9655-9662. https://doi.org/10.1021/ja001991j.

[94] L.M.C. Beltran, J.R. Long, Directed Assembly of Metal−Cyanide Cluster Magnets, Acc. Chem. Res. 38 (2005) 325-334. https://doi.org/10.1021/ar040158e

[95] T. Sanada, T. Suzuki, T. Yoshida, S. Kaizaki, heterodinuclear complexes containing d- and f-block elements: synthesis, structural characterization and metal-metal interactions of novel chromium(III)-lanthanide(III) compounds bridged by oxalate, Inorg. Chem. 37 (1998) 4712-4717. https://doi.org/10.1021/ic971568k.

[96] M.A. Subhan, T. Suzuki, S. Kaizaki, Stereospecific assembly of chiral Λ-Cr(III)-Δ-Ln(III) oxalato bridged dinuclear 3d-4f complexes (Ln = Yb, Dy) and near infrared dichroism in the 4f-4f transitions, J. Chem. Soc., Dalton Trans. (2001) 492-497. https://doi.org/10.1039/B007369P.

[97] M.A. Subhan, T. Suzuki, S. Kaizaki, Solution NIR CD and MCD in 4f-4f transitions of a series of chiral 3d-4f dinuclear complexes: X-ray structures of (D-L)-[(acac)2Cr(III)(m-ox)Ln(IIII)(HBpz3)2] (Ln = Sm, Ho, Er), J. Chem. Soc. Dalton Trans. (2002) 1416-1422. https://doi.org/10.1039/B108770C.

[98] M.A. Subhan, H. Nakata, T. Suzuki, J.-H. Choi, S. Kaizaki, Simultaneous observation of low temperature 4f-4f and 3d-3d emission spectra in a series of Cr(III)oxLn(III) assembly, J. of. Luminesc. 101 (2003) 307-315. https://doi.org/10.1016/S0022-2313(02)00573-2.

[99] M.A. Subhan, T. Suzuki, A. Fuyuhiro, S. Kaizaki, Synthesis, x-ray structures and NIR chirooptical properties of a series of dinuclear lanthanide(III) complexes Ln2(S-pba)4(hbpz)3; novel configurational chirality due to non-bonding Ln..O interactions, Dalton Trans. (2003) 3785-3791. https://doi.org/10.1039/B304928K.

[100] L. Andros, M. Juric, K. Molcanov, P. Planinic, Supramolecular architectures of novel chromium(III) oxalate complexes: steric effects of the ligand size and building-blocks approach, Dalton Trans., 41 (2012) 14611-14624. https://doi.org/10.1039/C2DT32249H.

[101] G. Marinescu, M. Andruh, F. Lloret, M. Julve, Bis(oxalato)chromium(III) complexes: Versatile tectons in designing heterometallic coordination compounds, Coord. Chem. Rev. 255 (2011) 161-185. https://doi.org/10.1016/j.ccr.2010.08.004.

[102] B. Doistau, J.-R. Jiménez, S. Guerra, C. Besnard, C. Piguet, Key Strategy for the Rational Incorporation of Long-Lived NIR Emissive Cr(III) Chromophores into Polymetallic Architectures, Inorg. Chem. 59 (2020) 1424-1435. https://doi.org/10.1021/acs.inorgchem.9b03163.

[103] H. D. Gafney, A. W. Adamson, Excited state $[Ru(bipyr)_3]^{2+}$ as an electron-transfer reductant, J. Am. Chem. Soc. 94 (1972) 8238-8239. https://doi.org/10.1021/ja00778a054.

[104] T. J. Meyer, Photochemistry of metal coordination complexes: metal to ligand charge transfer excited states, Pure Appl. Chem. 58 (1986) 1193-1206. http://dx.doi.org/10.1351/pac198658091193.

[105] V. Balzani, A. Juris, M. Venturi, S. Campagna, S. Serroni, Luminescent and redox-active polynuclear transition metal complexes, Chem. Rev. 96 (1996) 759-833. https://doi.org/10.1021/cr941154y.

[106] V. Balzani, A. Juris, Photochemistry and photophysics of Ru(II)-polypyridine complexes in the Bologna group. From early studies to recent developments, Coord. Chem. Rev. 211 (2001) 97-115. https://doi.org/10.1016/S0010-8545(00)00274-5.

[107] J. F. Endicott, H. B. Schlegel, M. J. Uddin, D. S. Seniveratne, MLCT excited states and charge delocalization in some ruthenium-ammine-polypyridyl complexes, Coord. Chem. Rev. 229 (2002) 95-106. https://doi.org/10.1016/S0010-8545(02)00105-4.

[108] V. Balzani, G. Bergamini, F. Marchioni, P. Ceroni, Ru(II)-bipyridine complexes in supramolecular systems, devices and machines, Coord. Chem. Rev. 250 (2006) 1254-1266, https://doi.org/10.1016/j.ccr.2005.11.013.

[109] V. Balzani, A. Credi, M. Venturi, Light powered molecular machines, Chem. Soc. Rev. 38 (2009) 1542-1550. https://doi.org/10.1039/B806328C.

[110] P. Ceroni, A. Credi, M. Venturi, Light to investigate (read) and operate (write) molecular devices and machines, Chem. Soc. Rev. 43 (2014) 4068-4083. https://doi.org/10.1039/C3CS60400D.

[111] X. Ma, E.A. Suturina, M. Rouziè, F. Wilhelm, A. Rogalev, R. Clérac, P. Dechambenoit, A heteroleptic diradical Cr(III) complex with extended spin delocalization and large intramolecular magnetic exchange, Chem. Commun. 56 (2020) 4906–4909. https://doi.org/10.1039/d0cc00548g.

[112] J.-R. Jiménez, B. Doistau, C.M. Cruz, C. Besnard, J.M. Cuerva, A.G. Campaña, C. Piguet, Chiral Molecular Ruby [Cr(dqp)2]3+ with Long-Lived Circularly Polarized Luminescence. J. Am. Chem. Soc. 141 (2019) 13244-13252. https://doi.org/10.1021/jacs.9b06524.

[113] S. Treiling, C. Wang, C. Förster, F. Reichenauer, J. Kalmbach, P. Boden, J.P. Harris, L.M. Carrella, E. Rentschler, U. Resch-Genger, C. Reber, M. Seitz, M. Gerhards, K. Heinze, Luminescence and Light-driven Energy and Electron Transfer from an Exceptionally Long-Lived Excited State of a

Non-innocent Chromium(III) Complex, Angew. Chem. Int. Ed. 58 (2019) 18075-18085. https://doi.org/10.1002/anie.201909325.

[114] A.B.P. Lever, Inorganic Electronic Spectroscopy; Elsevier, Amsterdam-Oxford-New York-Tokyo, 1984.

[115] G.E. Rojas, D. Magde, Temperature dependence of the doublet lifetime in chromium(III) compounds, Inorg. Chem. 26 (1987) 2334-2337. https://doi.org/10.1021/ic00261a034.

[116] M.W. Perkovic, M.J. Heeg, J.F. Endicott, Stereochemical perturbations of the relaxation behavior of (2E)chromium(III). Ground-state X-ray crystal structure, photophysics, and molecular mechanics simulations of the quasi-cage complex [4,4',4"-ethylidynetris(3-azabutan-1-amine)]chromium tribromide, Inorg. Chem. 30 (1991) 3140-3147. https://doi.org/10.1021/ic00016a009.

[117] C.K. Ryu, J.F. Endicott, Synthesis, Spectroscopy, and Photophysical Behavior of Mixed-Ligand Mono- and Bis(polypyridyl)chromium(III) Complexes. Examples of Efficient, Thermally Activated Excited-State Relaxation without Back Intersystem Crossing, Inorg. Chem. 27 (1988) 2203-2214. https://doi.org/10.1021/ic00286a002.

[118] A.M. McDaniel, H.-W. Tseng, N.H. Damrauer, M.P. Shores. Synthesis and solution phase characterization of strongly photooxidizing heteroleptic Cr(III) tris-dipyriyl complexes, Inorg. Chem. 49 (2010) 7981-7991. https://doi.org/10.1021/ic1009972.

[119] M. Isaacs, A.G. Sykes, S. Ronco, Synthesis, characterization and photophysical properties of mixed ligand tris(polypyridyl)chromium(III) complexes, [Cr(phen)2L]3+, Inorg. Chim. Acta 359 (2006) 3847-3854. https://doi.org/10.1016/j.ica.2006.04.036.

[120] J.C. Barbour, A.J.I. Kim, E. deVries, S.E. Shaner, B.M. Lovaasen, Chromium(III) Bis-Arylterpyridyl Complexes with Enhanced Visible Absorption via Incorporation of Intraligand Charge-Transfer Transitions, Inorg. Chem. 56 (2017) 8212-8222. https://doi.org/10.1021/acs.inorgchem.7b00953.

[121] C. Wang, S. Otto, M. Dorn, E. Kreidt, J. Lebon, L. Sršan, P. Di Martino-Fumo, M. Gerhards, U. Resch-Genger, M. Seitz, K. Heinze, Deuterated Molecular Ruby with Record Luminescence Quantum Yield. Angew. Chem. Int. Ed. 57 (2017) 1112-1116. https://doi.org/10.1002/anie.201711350

[122] C. Dee, F. Zinna, W.R. Kitzmann, G. Pescitelli, K. Heinze, L. Di Bari, M. Seitz, Strong circularly polarized luminescence of an octahedral chromium(III) complex, Chem. Commun. 55 (2019) 13078-13081. https://doi.org/10.1039/C9CC06909G.

[123] G. Sipos, R. Dorta, Iridium complexes with monodentate N-heterocyclic carbene ligands, Coord. Chem. Rev. 375 (2018) 13-68. https://doi.org/10.1016/j.ccr.2017.10.019

Graphical abstract

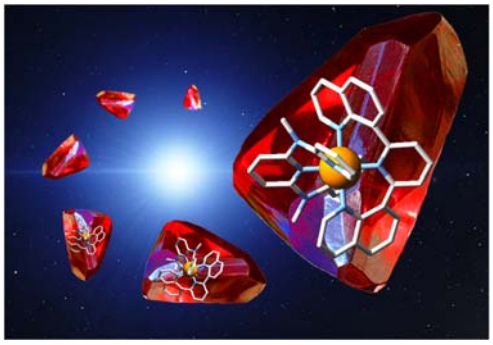

Tailored heteroleptic trivalent chromium complexes combine kinetic inertness and structural control with tuneable photophysical properties, all aspects which are crucial for the design of a next gereneration of cheap (supra)molecular light-converting assemblies and devices.